Hyper-Rayleigh scattering optical activity: theory, symmetry considerations and quantum chemistry applications

Andrea Bonvicini,[1] Kayn A. Forbes,[2] David L. Andrews,[2] and Benoît Champagne[1]
[1)]*Theoretical Chemistry Laboratory, Unit of Theoretical and Structural Physical Chemistry, Namur Institute of Structured Matter, University of Namur, B-5000 Namur, Belgium*
[2)]*School of Chemistry, University of East Anglia, Norwich Research Park, Norwich NR4 7TJ, United Kingdom*

(*benoit.champagne@unamur.be)

(*d.l.andrews@uea.ac.uk)

(*k.forbes@uea.ac.uk)

(*andrea.bonvicini@unamur.be)

(Dated: 18 April 2023)

This work reports on the first computational quantum-chemistry implementation of the hyper-Rayleigh scattering optical activity (HRS-OA), a nonlinear chiroptical phenomenon. First, from the basics of the theory, which is based on quantum electrodynamics, and focusing on the electric dipole, magnetic-dipole, and electric-quadrupole interactions, the equations for the simulation of the differential scattering ratios of HRS-OA are re-derived. Then, for the first time, computations of HRS-OA quantities are presented and analyzed. They have been enacted on a prototypical chiral organic molecule (methyloxirane) at the time-dependent density functional theory (TDDFT) level, using a broad range of atomic orbital basis sets. In particular, i) we analyze the basis set convergence, demonstrating that converged results require basis sets with both diffuse and polarization functions, ii) we discuss the relative amplitudes of the 5 contributions to the differential scattering ratios, and iii) we study the effects of origin-dependence and derived the expression of the tensor shifts and we prove the origin-independence of the theory for exact wavefunctions. Our computations show the ability of HRS-OA as a nonlinear chiroptical method, able to distinguish between the enantiomers of the same chiral molecule.

I. INTRODUCTION

Chirality is an important property of molecules. By definition, a molecule is chiral if it is not super-imposable onto its mirror image[1]. Chiral molecules are also referred to be dissymmetric objects. The geometrical prerequisite for chirality is the absence of an improper rotation axis $\hat{S}_n$, of any order n, where $\hat{S}_1$ corresponds to a symmetry plane ($\hat{\sigma}$) and $\hat{S}_2$, to an inversion centre $\hat{i}$[2,3]. Consequently, chiral molecules can exist in two opposite forms that are mirror images of each other, the *left*- and the *right*-handed forms, called enantiomers. Chirality exists also at other levels: from subatomic (neutrinos) to universe (spiral galaxies) scales, but above all, chirality plays a crucial role at the molecular scale and is therefore an extensively studied phenomenon in the fields of chemistry, biochemistry, biology, catalysis and pharmacology. In fact, life is based on chiral biomolecules[4,5]. For example, natural amino acids are almost exclusively found in their *left*-hand form (L-amino acids, in biochemistry nomenclature)[6]. Chirality can also be present at the supramolecular level. For example, α-helices, one of the most important secondary structures of proteins, are *right*-handed helices (*left*-handed α-helices are rare in nature)[6]. The three major forms of DNA are the *right*-handed A-DNA, the *right*-handed B-DNA, and the *left*-handed Z-DNA[7]. This remarkable selectivity of nature is known as biological *homochirality*[4]. It is thus important to develop and apply methods capable of chiral discrimination. Chiral discrimination for crystals can be done by using X-ray diffraction experiments[8]. On the other hand, most of the chemistry actually occurs in liquid or gas phases. It is thus necessary to consider other techniques for chiral discrimination in the fluid phases. Although NMR is an achiral method, this spectroscopy is widely used for a chiral molecule in solution. However, the chiral discrimination is obtained either through the use of a chiral derivatizing or a chiral solvating agent[9].

When a solution contains an enantiomeric excess of a chiral molecule, the enantiomers of that molecule can be distinguished using different chiroptical spectroscopies[10]. These spectroscopies are based on the optical activity (OA) phenomena. In fact, in all chiroptical spectroscopies, two opposite enantiomers of the same molecule show the same degree of optical activity but with opposite signs[11]. Among the chiroptical spectroscopies that probe the electronic degrees of freedom of a chiral molecule we can find optical rotation (OR)[12], electronic circular dichroism (ECD)[13,14] and circularly polarized luminescence (CPL)[15]. On the other hand, chirality can also be detected by probing the vibrational degrees of freedom of a chiral molecule. Vibrational circular dichroism (VCD)[16] and Raman optical activity (ROA)[17] are two examples of vibrational chiroptical spectroscopies. OR and ECD are routinely used to determine the absolute configuration of chiral molecules, their enantiomeric purity, or the secondary structure of proteins in solution[10,18]. All these spectroscopies are linear optics techniques because the incident field interacts with matter by a one-photon interaction process and the total intensity of the signal depends linearly on the intensity of the incident field. Nevertheless, linear chiroptical techniques suffer from the fact that the chiral response is usually very small compared to the total achiral response.

With the invention of lasers, access to high-intensity light enabled the discovery of nonlinear optics (NLO)[19,20]. Two-photon (TPCD) and the three-photon (3PCD) circular dichroism are examples of nonlinear counterpart of ECD[21–25]. Sum frequency generation (SFG) and second-harmonic generation (SHG) of chiral surfaces are other recently developed nonlinear chiroptical techniques[26,27]. In comparison to linear chiroptical techniques, the advantages brought by NLO for the detection of chirality-related events lies in its high level of chiral sensitivity, surface-enhanced signals, and large excitation wavelengths.

In 1979 Andrews and Thirunamachandran published the theoretical foundations of a novel nonlinear chiroptical method, namely the hyper-Rayleigh scattering optical activity (HRS-OA)[28]. The same article contains also the theory concerning hyper-Raman optical activity[28]. HRS-OA can be viewed as the chiroptical counterpart of the hyper-Rayleigh scattering (HRS) phenomena[29]. Both HRS and HRS-OA are incoherent second-order NLO processes by which two photons with the same frequency ω interact with a non-centrosymmetric molecule to create a single photon at the second harmonics, i.e., at the frequency 2ω[29,30]. In HRS experiments the incident light is linearly polarized while in HRS-OA it is circularly polarized, which enables the detection of optical activity by chiral molecules.

The HRS-OA phenomenon has been observed only 40 years after its theoretical development. The first experimental evidence of HRS-OA was reported in 2019 by Collins and collaborators for liquid solutions of silver nanohelices[31–33]. In 2020, Verrault and collaborators measured the HRS-OA for aromatic oligoamide foldamers in solution[34]. This was the first application of HRS-OA spectroscopy on molecular systems. Moreover, in this article, the authors showed that the second-order NLO chiral differences (i.e., between a pair of enantiomers) attain $10^{-1}-10^{-2}$ of the total HRS signal, in deep contrast with the linear chiroptical contributions (which are of the order of $10^{-3}-10^{-4}$ for ECD)[34]. These pioneering works paved the way to the development of an effective nonlinear chiroptical method allowing for the discrimination of chiral molecular and supramolecular systems in solution with high-sensitivity and low incident energy. The use of low energy photons is important for biological samples which can be destroyed or altered by UV-Vis light. While in this paper we are interested in HRS-OA only for the second-harmonic, it should be noticed that higher harmonics are in principle possible[35,36]. In fact, the first observation of OA in third-harmonic Rayleigh scattering (THRS) (three incident photons of frequency ω generate a single emitted photon of frequency 3ω) was reported in 2021 by Ohnoutek and collaborators[37].

The correlation between the absolute configuration of a molecule and the signs obtained in experimental chiroptical spectra (like ECD) is not always direct when experimental references are missing. The identification of the correct enantiomer can however be facilitated by means of theoretical simulations (based on quantum chemistry calculations) of the chiroptical spectroscopy[38–44]. For this reason, we decided to implement the necessary equations for the simulation of HRS-OA experiments. In the first part of this paper we perform a re-derivation of the necessary equations that describe the molecular origin of HRS-OA phenomenon (using the seminal article by Andrews and Thirunamachandran as a starting point[28]). We show how these molecular responses correlate with the (measured) scattered intensities and with the experimental set-ups. In the second part, the gauge-origin dependence of the theory is discussed. Finally, in the last part, for the first time, the HRS-OA quantities of a chiral molecule are calculated using quantum chemistry methods (here, at the TD-DFT level) and analysed.

II. THEORY OF HRS-OA

In this section we discuss the theory of HRS-OA starting in the macroscopic frame, i.e., where the experiments are performed, then moving to the molecular frame, i.e., from where the observed scattered intensities originate.

A. Macroscopic frame

From a phenomenological point of view, the HRS-OA phenomenon is an incoherent elastic scattering process based on a three-photon mechanism exerted under non resonant conditions (Figure 1). In particular, two identical incident photons, $\mathbf{r}$ and $\mathbf{t}$, are absorbed (annihilated) by the molecule, thus populating a virtual excited state. This excitation is simultaneously followed by emission (creation) of a scattered photon $\mathbf{s}$ at the second harmonic. To completely define the state of the incident and the scattered photons, we employ the following notations:

$$\mathbf{r} \equiv {}^{\lambda}\mathbf{r}(\hat{\mathbf{k}}, \omega), \tag{1}$$

$$\mathbf{t} \equiv \mathbf{r}, \tag{2}$$

$$\mathbf{s} \equiv {}^{\mu}\mathbf{s}(\hat{\mathbf{k}}', \omega_\sigma = 2\omega), \tag{3}$$

where $\hat{\mathbf{k}}$ ($\hat{\mathbf{k}}'$), ω (ω_σ) and λ (μ) are the unitary wavevector, angular frequency and polarization state of the incident (scattered) photon, respectively. HRS-OA experiments measures the differential scattering ratio:

$$\Delta_\mu(\theta) = \frac{{}^{R}I_\mu(\theta) - {}^{L}I_\mu(\theta)}{{}^{R}I_\mu(\theta) + {}^{L}I_\mu(\theta)}, \quad \mu = \parallel, \perp, \tag{4}$$

where L/R refers to left/right circularly polarized incident light, θ is the convergence angle defined by $\cos(\theta) = -\hat{\mathbf{k}}\cdot\hat{\mathbf{k}}'$, and μ, the polarization of the scattered photon, is usually resolved into its parallel ($\parallel$) and perpendicular ($\perp$) components with respect to the scattering plane defined by the unitary wavevectors $\hat{\mathbf{k}}$ and $\hat{\mathbf{k}}'$ (Figure 2)[28,29]. From a theoretical and computational point of view, we are interested in the molecular origins of the scattered intensities present in eq. (4), their analytical dependence on the scattering angle θ, and on the polarization μ.

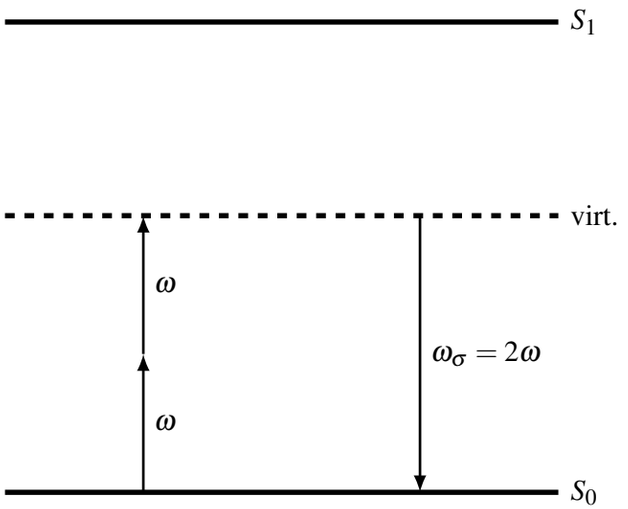

FIG. 1: The HRS-OA mechanism for two identical incident photons. Notice that the excitation with the two photons is not in a resonant or near-resonant region of the system (i.e., $2\omega \ll E(S_1) - E(S_0)$).

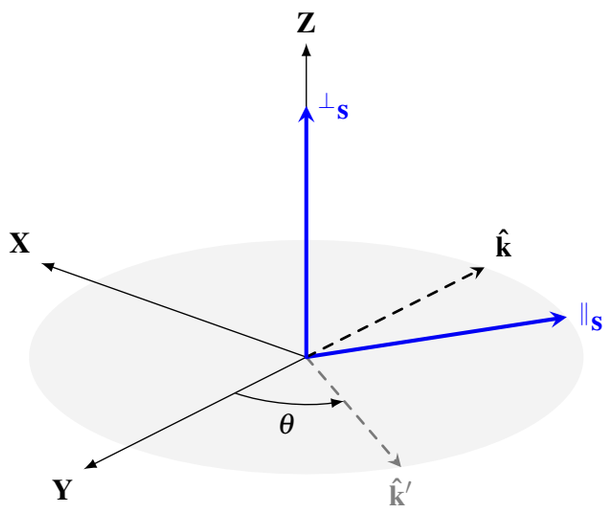

FIG. 2: The $(\mathbf{X},\mathbf{Y},\mathbf{Z})$ laboratory (macroscopic) frame adopted in this work. The figure also defines the scattering plane (in grey) and the scattering angle θ.

B. Molecular origins of HRS-OA

The theory of HRS-OA has been developed by Andrews and Thirunamachandran within the quantum electrodynamics (QED) framework and by employing the Power-Zienau-Woolley (PZW) multipolar Hamiltonian[45–52]. In QED, both the molecular and the radiation sub-systems are quantized. The PZW Hamiltonian of the total system reads[51]:

$$\hat{H} = (\hat{H}_{\rm mol} + \hat{H}_{\rm rad}) + \hat{H}_{\rm int} \equiv \hat{H}_0 + \hat{H}_{\rm int}, \tag{5}$$

where $\hat{H}_{\rm mol}$ is the molecular Hamiltonian, $\hat{H}_{\rm rad}$ is the Hamiltonian for the radiation field. Together they define the unperturbed Hamiltonian $\hat{H}_0$ whose eigenstates are the molecule-field product states $|{\rm mol}\rangle\,|{\rm rad}\rangle = |{\rm mol};{\rm rad}\rangle$ (Hilbert states for the material and Fock states for the field)[51]. The interaction Hamiltonian, $\hat{H}_{\rm int}$, describes the perturbations that allow transitions within the eigenstates of $\hat{H}_0$[51]. In general, the theoretical treatment of optical activity requires to go beyond the electric-dipole approximation in the interaction Hamiltonian[53]. In fact, for HRS-OA, the interaction Hamiltonian is[28,54]:

$$\hat{H}_{\rm int} = -(\varepsilon_0^{-1}\hat{\mu}_i\hat{d}_i^{\perp} + \hat{m}_i\hat{b}_i + \varepsilon_0^{-1}\hat{Q}_{ij}\nabla_j\hat{d}_i^{\perp}), \tag{6}$$

where $\hat{\boldsymbol{\mu}}$ and $\hat{\mathbf{Q}}$ are the electric-dipole and electric-quadrupole operators, respectively, and $\hat{\mathbf{m}}$ is the magnetic-dipole operator; $\hat{\mathbf{d}}^{\perp}$ is the transverse electric displacement field operator and $\hat{\mathbf{b}}$ is the magnetic field operator; i and j indices register Cartesian axes, $(\mathbf{X},\mathbf{Y},\mathbf{Z})$, of the macroscopic frame, ε_0 is the vacuum permittivity factor and the Einstein summation convention over repeated indices is adopted in eq. (6) and throughout this work. In eq. (6), the first term is the leading interaction term while the last two terms are usually two to three orders of magnitude smaller (a factor typically of the order of the fine structure constant α)[55].

The matrix element (quantum amplitude) for the HRS-OA phenomena, which is a three-photon process, can be obtained by third-order time-dependent perturbation theory[48,54]:

$$M_{fi} = \sum_{I,II} \frac{\langle f|\hat{H}_{\rm int}|II\rangle\langle II|\hat{H}_{\rm int}|I\rangle\langle I|\hat{H}_{\rm int}|i\rangle}{(E_i - E_{II})(E_i - E_I)} \tag{7}$$

where $|i\rangle$ and $|f\rangle$ are the initial and final states of the system (eigenstates of $\hat{H}_0$) while $|I\rangle$, $|II\rangle$ are intermediate states. The matrix elements for a process of any order can be obtained with the help of time-ordered (Feynman) diagrams[47–49,51,54,55]. By looking at eq. (6), it is clear that matrix elements containing mixed interaction types can appear in eq. (7). In fact, for HRS-OA phenomena, the matrix element contains five contributions[28]:

$$M_{fi} = M_{fi}(\beta) + M_{fi}({}^{\alpha}J) + M_{fi}({}^{\beta}J) + M_{fi}({}^{\alpha}K) + M_{fi}({}^{\beta}K). \tag{8}$$

The first matrix element in the rhs of eq. (8) contains three electric-dipole interactions and it is the dominant contribution to M_{fi}. It is also the leading (and unique) term in hyper-Rayleigh and in hyper-Raman scattering processes[29]. The second and the third matrix elements of eq. (8) contain two electric-dipole interactions and one magnetic-dipole interaction. The fourth and the fifth matrix elements of eq. (8) contain two electric-dipole interactions and one electric-quadrupole interaction. The last four terms in eq. (8) can be seen as corrections to the first[28].

The explicit expressions for the matrix elements present in eq. (8) are[28]:

$$M_{fi}(\beta) = -i\,d\,{}^{\mu}s_i\,{}^{L/R}r_j\,{}^{L/R}r_k\,\beta_{ijk}, \tag{9}$$

$$M_{fi}({}^{\alpha}J) = -i\,d\,(\hat{\mathbf{k}}'\times{}^{\mu}\mathbf{s})_i\,{}^{L/R}r_j\,{}^{L/R}r_k\,{}^{\alpha}J_{ijk}, \tag{10}$$

$$M_{fi}({}^{\beta}J) = -i\,d\,(\mp i)\,{}^{\mu}s_i\,{}^{L/R}r_j\,{}^{L/R}r_k\,{}^{\beta}J_{ijk}, \tag{11}$$

$$M_{fi}({}^{\alpha}K) = -\,d\,{}^{\mu}s_i\,{}^{L/R}r_j\,{}^{L/R}r_k\,k'_l\,{}^{\alpha}K_{ijkl}, \tag{12}$$

$$M_{fi}({}^{\beta}K) = d\,{}^{\mu}s_i\,{}^{L/R}r_j\,{}^{L/R}r_k\,k_l\,{}^{\beta}K_{ijkl}, \tag{13}$$

${}^{L/R}\mathbf{r}$ and ${}^{\mu}\mathbf{s}$ are the polarization vectors for the (two identical) incident and scattered photons, respectively, and $\hat{\mathbf{k}}$ and $\hat{\mathbf{k}}'$ are the unitary wavevector of the incident and scattered photons, respectively. In the r.h.s. of eqs. (9)-(13), the product between the elements of the polarization vectors and wavevectors defines the polarization tensor of the matrix elements. The last factor on the r.h.s of eqs. (9)-(13), is the molecular tensor of the matrix element. The tensor β_{ijk} is the pure electric-dipole (dynamic) first hyperpolarizability. The tensors ${}^{\alpha}J_{ijk}$ and ${}^{\beta}J_{ijk}$ are the mixed electric-dipole, electric-dipole, magnetic-dipole (dynamic) first hyperpolarizabilities. In ${}^{\alpha}J_{ijk}$ and ${}^{\beta}J_{ijk}$ the magnetic-dipole interaction is in emission and in absorption, respectively. The tensors ${}^{\alpha}K_{ijkl}$ and ${}^{\beta}K_{ijkl}$ are the mixed electric-dipole, electric-dipole, electric-quadrupole (dynamic) first hyperpolarizabilities. In ${}^{\alpha}K_{ijkl}$ and ${}^{\beta}K_{ijkl}$ the electric-quadrupole interaction is in emission and in absorption, respectively. In eq. (11) the upper and lower signs go with left (L) and right (R) circular polarization, respectively[28]. Finally, in eqs. (9)-(13) the prefactor d reads:

$$d = \left[\frac{8\pi^3\hbar^3\omega^2\omega_\sigma n(n-1)}{V^3}\right]^{1/2}, \tag{14}$$

where V is the quantization volume, n and $(n-1)$ are radiation-state numbers deriving from the quantization of the radiation field[49].

By looking at the expressions of the matrix elements, eqs. (9)-(13), one can notice that the polarization tensors are always (j,k)-symmetric, moreover, the polarization tensors are in (total) tensor contraction with the corresponding molecular tensors. Consequently, it is mathematically allowed to consider only the (j,k)-symmetric part of the molecular tensors β_{ijk}, ${}^{\alpha}J_{ijk}$, ${}^{\beta}J_{ijk}$, ${}^{\alpha}K_{ijkl}$, and ${}^{\beta}K_{ijkl}$[55–57]. This is the strategy adopted in the seminal article by Andrews and Thirunamachandran[28] and it is adopted in this work also. Moreover, because of the symmetry properties of the electric-quadrupole operator, the ${}^{\alpha}K_{ijkl}$ tensor is also symmetric and traceless in its (i,l)-indices, *vide infra*. Finally, from here, in the following, the indices of the molecular tensors will be indicated by Greek letters ($\alpha,\beta,\gamma,\delta$ or $\lambda,\mu,\nu,o,\pi,\rho,\sigma$) to emphasize the fact that they belong to the molecular frame.

The molecular tensors in eqs. (9)-(13) can be obtained from response theory[58,59]. It is important to emphasize that their detailed forms are fully consistent with those delivered by response theory, which is based on a semiclassical approach of light-matter interactions[59]. Ongoing from the QED framework to response theory is not straightforward and considerable intricacies need to be taken into account[51,55].

Using the language of response theory, one can associate the different dynamic first hyperpolarizabilities present in eqs. (9)-(13) to specific cases of a generic quadratic response function. In response theory, and by using the B-convention[60,61], the expression for a generic quadratic response function is[58,62–64]:

$$\langle\langle\hat{A}_\alpha;\hat{B}_\beta,\hat{C}_\gamma\rangle\rangle_{\omega_1,\omega_2} = \frac{1}{2}\sum\mathscr{P}_{-\sigma,1,2}\sum_{m,n}{}'\frac{A^{0m}_{\alpha}\overline{B}^{mn}_{\beta}C^{n0}_{\gamma}}{(E_{m0}-E_\sigma)(E_{n0}-E_2)}, \tag{15}$$

where $\hat{A}$, $\hat{B}$ and $\hat{C}$ are quantum-mechanical operators, ω_1 and ω_2 are the frequencies of the two incident photons and they are associated with the operators $\hat{B}$ and $\hat{C}$, respectively, and $\omega_\sigma = \omega_1+\omega_2$. In HRS-OA, $\omega_1=\omega_2=\omega$. Moreover, $E_{m0} = E_m - E_0$ and $E_\sigma = \hbar\omega_\sigma$. The notation $A^{0m}_{\alpha}\overline{B}^{mn}_{\beta}C^{n0}_{\gamma}$ is a shorthand notation for $\langle 0|\hat{A}_\alpha|m\rangle\langle m|\overline{\hat{B}_\beta}|n\rangle\langle n|\hat{C}_\gamma|0\rangle$ where $\overline{\hat{B}_\beta}$ is the fluctuation of the operator $\hat{B}$ and it is equal to $\hat{B}_\beta - \langle 0|\hat{B}_\beta|0\rangle$. The subscripts α, β, and γ register a generic Cartesian axis of the microscopic frame (x,y,z), $|0\rangle$ is the ground electronic state, while $|m\rangle$ and $|n\rangle$ are excited electronic states and the prime next to the summation symbol excludes the ground state from the summation (i.e., $|m\rangle$ and $|n\rangle \neq |0\rangle$). Finally, the operator $\mathscr{P}_{-\sigma,1,2}$ generates the permutation of the operator-frequency pairs ($\hat{A}_\alpha$, $-\omega_\sigma$), ($\hat{B}_\beta$, ω_1), and ($\hat{C}_\gamma$, ω_2), thus generating a total of 6 permutations.

Following the article by Andrews and Thirunamachandran, by performing suitable substitutions on the operators $\hat{A}$, $\hat{B}$, and $\hat{C}$ in eq. (15) one can obtain the expression for the hyperpolarizabilities in eqs. (9)-(13):

$$\beta_{\alpha\beta\gamma} = \langle\langle\hat{\mu}_\alpha;\hat{\mu}_\beta,\hat{\mu}_\gamma\rangle\rangle_{\omega,\omega}, \tag{16}$$

$${}^{\alpha}J_{\alpha\beta\gamma} = \langle\langle\hat{m}_\alpha;\hat{\mu}_\beta,\hat{\mu}_\gamma\rangle\rangle_{\omega,\omega}, \tag{17}$$

$${}^{\beta}J_{\alpha\beta\gamma} = \langle\langle\hat{\mu}_\alpha;\hat{m}_\beta,\hat{\mu}_\gamma\rangle\rangle_{\omega,\omega} + \langle\langle\hat{\mu}_\alpha;\hat{\mu}_\beta,\hat{m}_\gamma\rangle\rangle_{\omega,\omega} \tag{18}$$

$${}^{\alpha}K_{\alpha\beta\gamma\delta} = \langle\langle\hat{Q}_{\alpha\delta};\hat{\mu}_\beta,\hat{\mu}_\gamma\rangle\rangle_{\omega,\omega}, \tag{19}$$

$${}^{\beta}K_{\alpha\beta\gamma\delta} = \langle\langle\hat{\mu}_\alpha;\hat{Q}_{\beta\delta},\hat{\mu}_\gamma\rangle\rangle_{\omega,\omega} + \langle\langle\hat{\mu}_\alpha;\hat{\mu}_\beta,\hat{Q}_{\gamma\delta}\rangle\rangle_{\omega,\omega} \tag{20}$$

In eqs. (16)-(18), $\hat{\mu}_\alpha$, $\hat{m}_\alpha$ and $\hat{Q}_{\alpha\beta}$ are the electric-dipole moment, the magnetic-dipole moment, and the electric-quadrupole moment operators, respectively. These are given by[55,62,65–69]:

$$\hat{\mu}_\alpha = \sum_i q_i\hat{r}_{\alpha,i}, \tag{21}$$

$$\hat{m}_\alpha = \frac{1}{2c}\sum_i\frac{q_i}{m_i}\hat{l}_{\alpha,i} = \frac{1}{2c}\sum_i\frac{q_i}{m_i}\varepsilon_{\alpha\beta\gamma}(\hat{r}_\beta\hat{p}_\gamma)_i, \tag{22}$$

$$\hat{Q}_{\alpha\beta} = \frac{1}{2}\sum_i q_i(\hat{r}_{\alpha,i}\hat{r}_{\beta,i} - \frac{1}{3}\hat{r}_{\gamma,i}\hat{r}_{\gamma,i}\delta_{\alpha\beta}), \tag{23}$$

where q_i and m_i are the charge and the mass of i-th particle, respectively, $\hat{r}_{\alpha,i}$, $\hat{p}_{\alpha,i}$ ($=-i\hbar(\partial/\partial r_{\alpha,i})$) and $\hat{l}_{\alpha,i}$ are the position, the linear momentum, and the angular momentum operators in a generic Cartesian direction α of the molecular frame ($\alpha\in(x,y,z)$) for the i-th particle, respectively; $\varepsilon_{\alpha\beta\gamma}$ is the Levi-Civita tensor and c is the speed of light ($c=(1/\alpha)a_0E_\mathrm{h}/\hbar\approx 137$ in atomic units). For electrons and atomic units we have $m_e=\hbar=e=E_\mathrm{h}=1$ and $q_e=-e$ where e is the unit charge. In eq. (21) we used the length representation for the electric-dipole operator $\hat{\mu}_\alpha$. For real electronic wavefunctions and for non-resonant conditions, the integrals $\langle m|\hat{\mu}_\alpha|n\rangle$ are real while the integrals $\langle m|\hat{m}_\alpha|n\rangle$ are

imaginary[28]. Consequently, as we are in non-resonant conditions, the $\beta_{\alpha\beta\gamma}$, ${}^{\alpha}K_{\alpha\beta\gamma\delta}$, and ${}^{\beta}K_{\alpha\beta\gamma\delta}$ tensors are real, while the mixed electric-dipole magnetic-dipole first hyperpolarizabilities, i.e., the ${}^{\alpha}J_{\alpha\beta\gamma}$ and ${}^{\beta}J_{\alpha\beta\gamma}$ tensors, are imaginary[28].
All the molecular tensors in eqs. (16)-(20) are (β,γ)-symmetric. In particular, for two identical incident photon frequencies, the response functions for $\beta_{\alpha\beta\gamma}$, ${}^{\alpha}J_{\alpha\beta\gamma}$, and ${}^{\alpha}K_{\alpha\beta\gamma\delta}$ molecular tensor are intrinsically (β,γ)-symmetric. On the other hand, the response functions for the ${}^{\beta}J_{\alpha\beta\gamma}$, and ${}^{\beta}K_{\alpha\beta\gamma\delta}$ tensors have been symmetrized. Indeed, it is important to notice that if the operators $\hat{B}$ and $\hat{C}$ are not identical, eq. (15) does not generate a (β,γ)-symmetric tensor even for two identical incoming photons frequencies, i.e., $\langle\langle\hat{A}_\alpha;\hat{B}_\beta,\hat{C}_\gamma\rangle\rangle_{\omega,\omega} \neq \langle\langle\hat{A}_\alpha;\hat{B}_\gamma,\hat{C}_\beta\rangle\rangle_{\omega,\omega}$. However, as said before, ${}^{\beta}J_{\alpha\beta\gamma}$ must be symmetric in its (β,γ) indices[28]. For this reason, we used eq. (18) to symmetrize the ${}^{\beta}J_{\alpha\beta\gamma}$ quantities. Moreover, thanks to the permutation properties of quadratic response functions, for two identical incoming photons frequencies we can re-write eq. (18) as:

$$ {}^{\beta}J_{\alpha\beta\gamma} = \langle\langle\hat{\mu}_\alpha;\hat{\mu}_\beta,\hat{m}_\gamma\rangle\rangle_{\omega,\omega} + \langle\langle\hat{\mu}_\alpha;\hat{\mu}_\gamma,\hat{m}_\beta\rangle\rangle_{\omega,\omega}. \tag{24}$$

This means that ${}^{\beta}J_{\alpha\beta\gamma}$ symmetric in its (β,γ)-indices can be obtained from a single quadratic response function symmetrized in its (β,γ)-indices.
The symmetrization of the ${}^{\beta}K_{\alpha\beta\gamma\delta}$ tensor suffers from the same problem as the ${}^{\beta}J_{\alpha\beta\gamma}$ tensor does. In fact, also in this case, the two light-matter interactions in the absorption process for ${}^{\beta}K_{\alpha\beta\gamma\delta}$ are not identical, i.e., $\hat{B}\neq\hat{C}$. Using similar arguments adopted in the previous paragraph, the ${}^{\beta}K_{\alpha\beta\gamma\delta}$ tensor symmetric in its (β,γ)-indices is obtained as the sum of two tensors, see eq. (20). The first tensor in the r.h.s. of eq. (20) is obtained from eq. (16) with $\hat{\mu}_\beta \to \hat{Q}_{\beta\delta}$, while the second tensor in the r.h.s. of eq. (20) is obtained from eq. (16) with $\hat{\mu}_\gamma \to \hat{Q}_{\gamma\delta}$. This procedure is used in ref.[28].
Finally, as done before, thanks to the permutation properties of the quadratic response functions, for two identical incoming photons we can re-write eq. (20) as:

$$ {}^{\beta}K_{\alpha\beta\gamma\delta} = \langle\langle\hat{\mu}_\alpha;\hat{\mu}_\gamma,\hat{Q}_{\beta\delta}\rangle\rangle_{\omega,\omega} + \langle\langle\hat{\mu}_\alpha;\hat{\mu}_\beta,\hat{Q}_{\gamma\delta}\rangle\rangle_{\omega,\omega} \tag{25}$$

This means that ${}^{\beta}K_{\alpha\beta\gamma\delta}$ symmetric in its (β,γ)-indices can be obtained from a single quadratic response function symmetrized in its (β,γ)-indices.

C. The scattered intensities

By applying the Fermi golden rule, it emerges that each intensity term in eq. (4) is given by five different contributions[28]:

$$ I = \frac{|k'|^3 VN}{4\pi\hbar}\cdot\langle|M_{fi}(\beta)+M_{fi}({}^{\alpha}J)+M_{fi}({}^{\beta}J)+M_{fi}({}^{\alpha}K)+M_{fi}({}^{\beta}K)|^2\rangle \tag{26}$$

and

$$ I \approx I(\langle\beta^2\rangle)+I(\langle\beta^{\alpha}J\rangle)+I(\langle\beta^{\beta}J\rangle)+I(\langle\beta^{\alpha}K\rangle)+I(\langle\beta^{\beta}K\rangle). \tag{27}$$

where N is the number of scatters of the sample and the symbol $\langle\rangle$ denotes rotational averaged quantities (HRS-OA experiments are performed in the fluid phase). The first term in the rhs of eq (27) is the dominant contribution to the total scattered intensity and it is always positive. The next four terms are corrections (interferences) and can be either positive or negative. Ongoing from eq. (26) to eq. (27), the small terms containing interferences between the matrix elements of the mixed interactions have been neglected. The explicit expressions for the scattered intensities appearing in eq. (27) are:

$$ I(\langle\beta^2\rangle) = D\, s_i{}^{L/R} e_j{}^{L/R} e_k\, s_l{}^{R/L} e_m{}^{R/L} e_n\, \beta_{\lambda\mu\nu}\beta_{o\pi\rho}\, I^{(6)}_{ijklmn;\lambda\mu\nu o\pi\rho}, \tag{28}$$

$$ I(\langle\beta^{\alpha}J\rangle) = -2\, D\, s_i{}^{L/R} e_j{}^{L/R} e_k\, (\hat{\mathbf{k}}'\times\mathbf{s})_l{}^{R/L} e_m{}^{R/L} e_n\, \beta_{\lambda\mu\nu}{}^{\alpha}J_{o\pi\rho}\, I^{(6)}_{ijklmn;\lambda\mu\nu o\pi\rho}, \tag{29}$$

$$ I(\langle\beta^{\beta}J\rangle) = -2\, D\, s_i{}^{L/R} e_j{}^{L/R} e_k\cdot(\pm i)\, s_l{}^{R/L} e_m{}^{R/L} e_n\, \beta_{\lambda\mu\nu}{}^{\beta}J_{o\pi\rho}\, I^{(6)}_{ijklmn;\lambda\mu\nu o\pi\rho}, \tag{30}$$

$$ I(\langle\beta^{\alpha}K\rangle) = 2i\, D\, s_i{}^{L/R} e_j{}^{L/R} e_k\, s_l{}^{R/L} e_m{}^{R/L} e_n\, k'_p\, \beta_{\lambda\mu\nu}{}^{\alpha}K_{o\pi\rho\sigma}\, I^{(7)}_{ijklmnp;\lambda\mu\nu o\pi\rho\sigma}, \tag{31}$$

$$ I(\langle\beta^{\beta}K\rangle) = -2i\, D\, s_i{}^{L/R} e_j{}^{L/R} e_k\, s_l{}^{R/L} e_m{}^{R/L} e_n\, k_p\, \beta_{\lambda\mu\nu}{}^{\beta}K_{o\pi\rho\sigma}\, I^{(7)}_{ijklmnp;\lambda\mu\nu o\pi\rho\sigma}, \tag{32}$$

where the prefactor D is:

$$ D = \frac{2\pi}{c} N|k'|^4 g^{(2)}\bar{I}_0^2. \tag{33}$$

where $g^{(2)}$ and $\bar{I}_0^2$ are the degree of second order coherence and mean irradiance of the incident beam, respectively. The

prefactor D is not further taken into account in the following work because it can be factorized in both numerator and denominator of eq. (4). In eqs. (28)-(30), $I^{(6)}_{ijklmn;\lambda\mu\nu o\pi\rho}$ and $I^{(7)}_{ijklmnp;\lambda\mu\nu o\pi\rho\sigma}$ are the isotropic tensors of rank 6 and rank 7, respectively[70]. In eq. (30), the upper and lower signs go with L-CPL and R-CPL, respectively. The presence of an isotropic tensor is necessary in order to obtain rotational-averaged scalar quantities (i.e., the scattered intensities). The mathematical details concerning the rotational averaging procedure for HRS-OA are provided in the Supporting Information (SI) file. The final expressions for the HRS-OA circular differential scattering ratios, eq. (4) are:

$$\Delta_{\parallel}(\theta) = \frac{a + b\cos(\theta) + c\cos^2(\theta) + d\cos^3(\theta)}{f + g\cos^2(\theta)}, \tag{34}$$

and

$$\Delta_{\perp}(\theta) = \frac{a + (b+d)\cos(\theta) + c}{f + g}, \tag{35}$$

where a, b, c, d, f and g terms contain the scalar molecular invariants of $I(\langle\beta^2\rangle)$, $I(\langle\beta^\alpha J\rangle)$, $I(\langle\beta^\beta J\rangle)$, $I(\langle\beta^\alpha K\rangle)$ and $I(\langle\beta^\beta K\rangle)$, and are given by:

$$\begin{aligned} a = &-4\,\mathrm{Im}(4\beta_{\lambda\lambda\mu}{}^{\beta}J_{\mu\nu\nu} - 6\beta_{\lambda\lambda\mu}{}^{\beta}J_{\nu\mu\nu} - 5\beta_{\lambda\mu\mu}{}^{\beta}J_{\lambda\nu\nu} + 4\beta_{\lambda\mu\mu}{}^{\beta}J_{\nu\lambda\nu} + 11\beta_{\lambda\mu\nu}{}^{\beta}J_{\lambda\mu\nu} - 6\beta_{\lambda\mu\nu}{}^{\beta}J_{\mu\lambda\nu}) \\ &+2|k|(4\beta_{\lambda\mu\mu}{}^{\beta}K_{o\pi o\sigma}\varepsilon_{\lambda\pi\sigma} - 5\beta_{\lambda\mu\mu}{}^{\beta}K_{o\pi\pi\sigma}\varepsilon_{\lambda o\sigma} + 6\beta_{\lambda\mu\mu}{}^{\beta}K_{o\pi\rho\rho}\varepsilon_{\lambda o\pi} - 10\beta_{\lambda\mu\nu}{}^{\beta}K_{ovo\sigma}\varepsilon_{\lambda\mu\sigma} \\ &+5\beta_{\lambda\mu\nu}{}^{\beta}K_{ov\mu\sigma}\varepsilon_{\lambda o\sigma} + 2\beta_{\lambda\mu\nu}{}^{\beta}K_{o\pi ov}\varepsilon_{\lambda\mu\pi} + 18\beta_{\lambda\mu\nu}{}^{\beta}K_{o\pi vo}\varepsilon_{\lambda\mu\pi} - 10\beta_{\lambda\mu\nu}{}^{\beta}K_{o\pi v\mu}\varepsilon_{\lambda o\pi} \\ &-4\beta_{\lambda\mu\nu}{}^{\beta}K_{o\pi\pi v}\varepsilon_{\lambda\mu o} + 6\beta_{\lambda\mu\nu}{}^{\beta}K_{v\pi\pi\sigma}\varepsilon_{\lambda\mu\sigma} - 8\beta_{\lambda\mu\nu}{}^{\beta}K_{v\pi\rho\rho}\varepsilon_{\lambda\mu\pi}) \end{aligned} \tag{36}$$

$$\begin{aligned} b = &-28\,\mathrm{Im}(\beta_{\lambda\lambda\mu}{}^{\alpha}J_{\nu\mu\nu} - \beta_{\lambda\mu\nu}{}^{\alpha}J_{\mu\lambda\nu}) \\ &+4|k'|(2\beta_{\lambda\mu\mu}{}^{\alpha}K_{o\pi\rho\rho}\varepsilon_{\lambda o\pi} - 3\beta_{\lambda\mu\nu}{}^{\alpha}K_{ov\rho\rho}\varepsilon_{\lambda\mu o} - 3\beta_{\lambda\mu\nu}{}^{\alpha}K_{o\pi v\mu}\varepsilon_{\lambda o\pi} \\ &+2\beta_{\lambda\mu\nu}{}^{\alpha}K_{o\pi\pi v}\varepsilon_{\lambda\mu o} - 6\beta_{\lambda\mu\nu}{}^{\alpha}K_{v\pi\rho\rho}\varepsilon_{\lambda\mu\pi}) \end{aligned} \tag{37}$$

$$\begin{aligned} c = &+4\,\mathrm{Im}(6\beta_{\lambda\lambda\mu}{}^{\beta}J_{\mu\nu\nu} - 9\beta_{\lambda\lambda\mu}{}^{\beta}J_{\nu\mu\nu} - 4\beta_{\lambda\mu\mu}{}^{\beta}J_{\lambda\nu\nu} + 6\beta_{\lambda\mu\mu}{}^{\beta}J_{\nu\lambda\nu} + 6\beta_{\lambda\mu\nu}{}^{\beta}J_{\lambda\mu\nu} - 9\beta_{\lambda\mu\nu}{}^{\beta}J_{\mu\lambda\nu}) \\ &+|k|(16\beta_{\lambda\mu\mu}{}^{\beta}K_{o\pi o\sigma}\varepsilon_{\lambda\pi\sigma} - 13\beta_{\lambda\mu\mu}{}^{\beta}K_{o\pi\pi\sigma}\varepsilon_{\lambda o\sigma} + 10\beta_{\lambda\mu\mu}{}^{\beta}K_{o\pi\rho\rho}\varepsilon_{\lambda o\pi} - 26\beta_{\lambda\mu\nu}{}^{\beta}K_{ovo\sigma}\varepsilon_{\lambda\mu\sigma} \\ &+13\beta_{\lambda\mu\nu}{}^{\beta}K_{ov\mu\sigma}\varepsilon_{\lambda o\sigma} + 28\beta_{\lambda\mu\nu}{}^{\beta}K_{ov\rho\rho}\varepsilon_{\lambda\mu o} + 22\beta_{\lambda\mu\nu}{}^{\beta}K_{o\pi ov}\varepsilon_{\lambda\mu\pi} - 26\beta_{\lambda\mu\nu}{}^{\beta}K_{o\pi vo}\varepsilon_{\lambda\mu\pi} \\ &+2\beta_{\lambda\mu\nu}{}^{\beta}K_{o\pi v\mu}\varepsilon_{\lambda o\pi} - 16\beta_{\lambda\mu\nu}{}^{\beta}K_{o\pi\pi v}\varepsilon_{\lambda\mu o} + 10\beta_{\lambda\mu\nu}{}^{\beta}K_{v\pi\pi\sigma}\varepsilon_{\lambda\mu\sigma} - 4\beta_{\lambda\mu\nu}{}^{\beta}K_{v\pi\rho\rho}\varepsilon_{\lambda\mu\pi}) \end{aligned} \tag{38}$$

$$\begin{aligned} d = &-2|k'|(5\beta_{\lambda\mu\mu}{}^{\alpha}K_{o\pi\rho\rho}\varepsilon_{\lambda o\pi} + 3\beta_{\lambda\mu\nu}{}^{\alpha}K_{ov\rho\rho}\varepsilon_{\lambda\mu o} + 3\beta_{\lambda\mu\nu}{}^{\alpha}K_{o\pi v\mu}\varepsilon_{\lambda o\pi} \\ &+5\beta_{\lambda\mu\nu}{}^{\alpha}K_{o\pi\pi v}\varepsilon_{\lambda\mu o} - 15\beta_{\lambda\mu\nu}{}^{\alpha}K_{v\pi\rho\rho}\varepsilon_{\lambda\mu\pi}) \end{aligned} \tag{39}$$

$$f = +2(8\beta_{\lambda\lambda\mu}\beta_{\mu\nu\nu} - 6\beta_{\lambda\lambda\mu}\beta_{\nu\mu\nu} - 5\beta_{\lambda\mu\mu}\beta_{\lambda\nu\nu} + 11\beta_{\lambda\mu\nu}\beta_{\lambda\mu\nu} - 6\beta_{\lambda\mu\nu}\beta_{\mu\lambda\nu}) \tag{40}$$

$$g = -2(12\beta_{\lambda\lambda\mu}\beta_{\mu\nu\nu} - 9\beta_{\lambda\lambda\mu}\beta_{\nu\mu\nu} - 4\beta_{\lambda\mu\mu}\beta_{\lambda\nu\nu} + 6\beta_{\lambda\mu\nu}\beta_{\lambda\mu\nu} - 9\beta_{\lambda\mu\nu}\beta_{\mu\lambda\nu}) \tag{41}$$

The a, b, c, d, f and g quantities are intensity terms and they contain the molecular invariants, which involve the molecular properties at the origin of the HRS-OA phenomena. In particular, the a and c terms contain scalar molecular invariants of $I(\langle\beta^\beta J\rangle)$ (a total of 6 invariants) and $I(\langle\beta^\beta K\rangle)$ (a total of 12 invariants, 11 in a and 12 in c), which are associated with different numerical coefficients. The b term contains molecular invariants of $I(\langle\beta^\alpha J\rangle)$ (a total of 2) and $I(\langle\beta^\alpha K\rangle)$ (a total of 5), the term d contains molecular invariants of $I(\langle\beta^\alpha K\rangle)$ (a total of 5) and finally, f and g terms contain molecular invariants from $I(\langle\beta^2\rangle)$ (both contain a total of 5 invariants). Also in this case, the scalar molecular invariants in f and g are associated with different numerical coefficients.

Since they vanish for achiral molecules, we can identify the a,

b, c, and d terms as chiral contributions while f and g terms are achiral ones to eq. (34) and (35). It is interesting to notice that only two invariants of $I(\langle\beta^{\alpha}J\rangle)$ are contributing to the b term and, the analytic dependence on b is the same for $\Delta_{\parallel}(\theta)$ and $\Delta_{\perp}(\theta)$. Finally, the numerators of both eqs. (34) and (35) contain only the chiral terms a, b, c, and d which have contributions from the mixed electric-magnetic dipole or mixed electric-dipole electric-quadrupole interactions. This means that the pure electric-dipole contribution (β^2 terms) is independent on the handedness of incident photons and has no contribution in the numerator of eq. (4). In fact, the denominators in eqs. (34) and (35) contain only f and g terms, associated only with the pure electric first hyperpolarizability β. This means that for R- and L-CPL the $\beta^{\alpha}J$, $\beta^{\beta}J$, $\beta^{\alpha}K$, and $\beta^{\beta}K$ contributions for each polarization cancel out in the denominator.

Another important fact is that the invariants of $I(\langle\beta^{\alpha}K\rangle)$ and $I(\langle\beta^{\beta}K\rangle)$ are scaled by $|k'|$ and $|k|$, respectively, i.e., the magnitude of the wavevectors for the emitted and the absorbed photons ($|k'| = 2|k|$). This means that close to the static limit (i.e., at low frequencies) their impact could be considered negligible.

It is important to notice that when the wavevectors $\hat{\mathbf{k}}$ and $\hat{\mathbf{k}}'$ point in the same or in opposite directions (i.e., when $\theta = 180°$ or $0°$, respectively) then $\Delta_{\parallel}$ and $\Delta_{\perp}$ are identical.

D. The origin dependence

The calculated molecular properties should be independent of the choice of the gauge origin (**O**). This requirement is automatically fulfilled when the one-electron basis is complete. For truncated basis sets origin independence is not guaranteed[71]. If one changes the Cartesian origin $\mathbf{O} \rightarrow \mathbf{O}' = \mathbf{O} + \mathbf{R}$ one obtains the following shift on the position operator for the i-th particle:

$$\hat{\mathbf{r}}_i \rightarrow \hat{\mathbf{r}}'_i = \hat{\mathbf{r}}_i - \mathbf{R}. \tag{42}$$

This change in the gauge-origin is reflected into the quantum mechanical operators. For example, the electric-dipole operator changes as[69]:

$$\hat{\mu}_{\alpha} \rightarrow \hat{\mu}'_{\alpha} = \hat{\mu}_{\alpha} - R_{\alpha}\sum_i q_i. \tag{43}$$

For neutral systems, a change in the gauge origin does not affect $\hat{\mu}_{\alpha}$ (in fact, $\sum_i q_i = 0$). Consequently, the pure-electric properties like, the linear and nonlinear (hyper)polarizabilites ($\alpha_{\alpha\beta}$, $\beta_{\alpha\beta\gamma}$, $\gamma_{\alpha\beta\gamma\delta}$, etc...) are origin-independent even for computations with finite basis sets. For charged species, the origin independence is guaranteed by the fluctuation dipole operator, $\overline{\hat{B}_{\beta}}$, in eq. (15). Upon change in the gauge-origin **O**, the shift on the magnetic-dipole operator reads[69]:

$$\begin{aligned}\hat{m}_{\alpha} \rightarrow \hat{m}'_{\alpha} &= \hat{m}_{\alpha} - \sum_i \frac{q_i}{2m_i c}\varepsilon_{\alpha\beta\gamma}R_{\beta}\hat{p}_{\gamma,i} \\ &= \hat{m}_{\alpha} - \frac{1}{2c}\varepsilon_{\alpha\beta\gamma}R_{\beta}\hat{\mu}^{p}_{\gamma},\end{aligned} \tag{44}$$

where

$$\hat{\mu}^{p}_{\gamma} = \sum_i \frac{q_i}{m_i}\hat{p}_{\gamma,i}, \tag{45}$$

is the electric-dipole operator in the so-called velocity form[72]. This shift propagates into the mixed electric-magnetic dipole first hyperpolarizabilities ${}^{\alpha}J_{\lambda\mu\nu}$ and ${}^{\beta}J_{\lambda\mu\nu}$. In particular, the shift in ${}^{\alpha}J_{\lambda\mu\nu}$ reads:

$${}^{\alpha}J_{\lambda\mu\nu} \rightarrow {}^{\alpha}J'_{\lambda\mu\nu} = {}^{\alpha}J_{\lambda\mu\nu} + \Delta({}^{\alpha}J_{\lambda\mu\nu}) \tag{46}$$

where

$$\Delta({}^{\alpha}J_{\lambda\mu\nu}) = -\frac{1}{2c}\varepsilon_{\lambda\beta\gamma}R_{\beta}\langle\langle\hat{\mu}^{p}_{\gamma};\hat{\mu}_{\mu},\hat{\mu}_{\nu}\rangle\rangle, \tag{47}$$

At the same time, the shift in ${}^{\beta}J_{\lambda\mu\nu}$ reads:

$${}^{\beta}J_{\lambda\mu\nu} \rightarrow {}^{\beta}J'_{\lambda\mu\nu} = {}^{\beta}J_{\lambda\mu\nu} + \Delta({}^{\beta}J_{\lambda\mu\nu}) \tag{48}$$

where

$$\begin{aligned}\Delta({}^{\beta}J_{\lambda\mu\nu}) = &-\frac{1}{2c}\varepsilon_{\nu\beta\gamma}R_{\beta}\langle\langle\hat{\mu}_{\lambda};\hat{\mu}_{\mu},\hat{\mu}^{p}_{\gamma}\rangle\rangle \\ &-\frac{1}{2c}\varepsilon_{\mu\beta\gamma}R_{\beta}\langle\langle\hat{\mu}_{\lambda};\hat{\mu}_{\nu},\hat{\mu}^{p}_{\gamma}\rangle\rangle.\end{aligned} \tag{49}$$

Eqs. (46) and (48) show the linear dependence of the ${}^{\alpha}J_{\lambda\mu\nu}$ and ${}^{\beta}J_{\lambda\mu\nu}$ shifts on vector R. Consequently, the larger the diplacement vector **R**, the larger will be the shifts on the mixed electric-magnetic dipole first hyperpolarizabilites ${}^{\alpha}J_{\lambda\mu\nu}$ and ${}^{\beta}J_{\lambda\mu\nu}$. These shifts, eqs. (46) and (48), were then verified numerically; see Sec. III B 3 for further details. By using approximate wavefunctions and by using finite basis sets, the origin-dependence of the mixed electric-magnetic dipole first hyperpolarizabilities ${}^{\alpha}J_{\lambda\mu\nu}$ and ${}^{\beta}J_{\lambda\mu\nu}$ is present. This issue can be solved, for example, by using London atomic-orbitals (also named gauge independent atomic orbital, GIAO). In particular, the use of London orbitals ensures that the shifts in eq. (47) and eq. (49) will involve the electric-dipole operators in the length gauge only, even with finite basis sets, and these will exactly cancel with the origin dependences of the electric-quadrupole first hyperpolarizabilities, ${}^{\alpha}K_{\lambda\mu\nu o}$, and ${}^{\beta}K_{\lambda\mu\nu o}$, that are discussed in the next paragraph[71,73,74].

At the same time, the shift upon change in the gauge-origin on the traceless electric-quadrupole operator reads[67]:

$$\begin{aligned}\hat{Q}_{\alpha\beta} \rightarrow \hat{Q}'_{\alpha\beta} =&\hat{Q}_{\alpha\beta} + \sum_i(-\frac{1}{2}R_{\alpha}\hat{r}_{\beta,i}q_i - \frac{1}{2}R_{\beta}\hat{r}_{\alpha,i}q_i \\ &+\frac{1}{3}R_{\gamma}\hat{r}_{\gamma,i}q_i\delta_{\alpha\beta} + \frac{1}{2}R_{\alpha}R_{\beta}q_i - \frac{1}{6}R_{\gamma}R_{\gamma}q_i\delta_{\alpha\beta})\end{aligned} \tag{50}$$

For a neutral system, the last two terms in the right hand side of eq. (50) are zero because the vector **R** is not a quantum-mechanical operator (it is just a multiplicative factor of the system eigenfunctions) and, again, $\sum_i q_i = 0$. Consequently, for a neutral system, the shift on $\hat{Q}_{\alpha\beta}$ propagates into ${}^{\alpha}K_{\lambda\mu\nu o}$ as:

$${}^{\alpha}K_{\lambda\mu\nu o} \rightarrow {}^{\alpha}K'_{\lambda\mu\nu o} = {}^{\alpha}K_{\lambda\mu\nu o} + \Delta({}^{\alpha}K_{\lambda\mu\nu o}) \tag{51}$$

where

$$\Delta({}^{\alpha}K_{\lambda\mu\nu o}) = -\frac{1}{2}R_{\lambda}\langle\langle\hat{\mu}_o;\hat{\mu}_{\mu},\hat{\mu}_{\nu}\rangle\rangle - \frac{1}{2}R_o\langle\langle\hat{\mu}_{\lambda};\hat{\mu}_{\mu},\hat{\mu}_{\nu}\rangle\rangle + \frac{1}{3}R_{\gamma}\langle\langle\hat{\mu}_{\gamma};\hat{\mu}_{\mu},\hat{\mu}_{\nu}\rangle\rangle\delta_{\lambda o}. \tag{52}$$

At the same time, the shift in ${}^{\beta}K_{\lambda\mu\nu o}$ reads:

$${}^{\beta}K_{\lambda\mu\nu o} \rightarrow {}^{\beta}K'_{\lambda\mu\nu o} = {}^{\beta}K_{\lambda\mu\nu o} + \Delta({}^{\beta}K_{\lambda\mu\nu o}) \tag{53}$$

where

$$\begin{aligned}\Delta({}^{\beta}K_{\lambda\mu\nu o}) = &-\frac{1}{2}R_{\mu}\langle\langle\hat{\mu}_{\lambda};\hat{\mu}_{\nu},\hat{\mu}_o\rangle\rangle - \frac{1}{2}R_o\langle\langle\hat{\mu}_{\lambda};\hat{\mu}_{\nu},\hat{\mu}_{\mu}\rangle\rangle\\ &+\frac{1}{3}R_{\gamma}\langle\langle\hat{\mu}_{\lambda};\hat{\mu}_{\nu},\hat{\mu}_{\gamma}\rangle\rangle\delta_{\mu o}\\ &-\frac{1}{2}R_{\nu}\langle\langle\hat{\mu}_{\lambda};\hat{\mu}_{\mu},\hat{\mu}_o\rangle\rangle - \frac{1}{2}R_o\langle\langle\hat{\mu}_{\lambda};\hat{\mu}_{\mu},\hat{\mu}_{\nu}\rangle\rangle\\ &+\frac{1}{3}R_{\gamma}\langle\langle\hat{\mu}_{\lambda};\hat{\mu}_{\mu},\hat{\mu}_{\gamma}\rangle\rangle\delta_{\nu o}\end{aligned} \tag{54}$$

as for the previous case, the shift on the ${}^{\alpha}K_{\lambda\mu\nu o}$ and ${}^{\beta}K_{\lambda\mu\nu o}$ tensors are linearly dependent on the components of the displacement vector **R**. These shifts, eqs. (51) and (53), were then verified numerically; see Sec. III B 3 for further details.

1. The origin-independence of the theory for exact wavefunctions

The theory of HRS-OA can be proved to be origin-independent for exact wavefuntion if one consider the following commutator[72]:

$$[\hat{\mu}_{\alpha},\hat{H}_{\mathrm{mol}}] = i\hat{\mu}^{p}_{\alpha}, \tag{55}$$

and the following relations for the quadratic response functions[58,72,75]:

$$\omega_{\sigma}\langle\langle\hat{\mu}_{\lambda};\hat{\mu}_{\mu},\hat{\mu}_{\nu}\rangle\rangle_{\omega_1,\omega_2} = i\langle\langle\hat{\mu}^{p}_{\lambda};\hat{\mu}_{\mu},\hat{\mu}_{\nu}\rangle\rangle_{\omega_1,\omega_2} \tag{56}$$

and

$$\omega_2\langle\langle\hat{\mu}_{\lambda};\hat{\mu}_{\mu},\hat{\mu}_{\nu}\rangle\rangle_{\omega_1,\omega_2} = -i\langle\langle\hat{\mu}_{\lambda};\hat{\mu}_{\mu},\hat{\mu}^{p}_{\nu}\rangle\rangle_{\omega_1,\omega_2}, \tag{57}$$

which are valid for exact wavefunctions and variational wavefunctions in the limit of a complete basis set. For HRS-OA, $\omega_1 = \omega_2 = \omega$, and $\omega_{\sigma} = 2\omega$. Consequently, eq. (56), and eq. (57) enable one to re-write the $\Delta({}^{\alpha/\beta}J_{\lambda\mu\nu})$ shifts appearing in eq. (47) and in eq. (49) with the full-length form of the electric-dipole first hyperpolarizability (i.e., $\beta_{\lambda\mu\nu}$):

$$\begin{aligned}\Delta({}^{\alpha}J_{\lambda\mu\nu}) &= \frac{1}{2c}\varepsilon_{\lambda\beta\gamma}R_{\beta}2\omega i\langle\langle\hat{\mu}_{\gamma};\hat{\mu}_{\mu},\hat{\mu}_{\nu}\rangle\rangle\\ &= \frac{1}{2}|k'|\varepsilon_{\lambda\beta\gamma}R_{\beta}i\langle\langle\hat{\mu}_{\gamma};\hat{\mu}_{\mu},\hat{\mu}_{\nu}\rangle\rangle,\end{aligned} \tag{58}$$

and

$$\begin{aligned}\Delta({}^{\beta}J_{\lambda\mu\nu}) &= -\frac{1}{2c}\varepsilon_{\nu\beta\gamma}R_{\beta}\omega i\langle\langle\hat{\mu}_{\lambda};\hat{\mu}_{\mu},\hat{\mu}_{\gamma}\rangle\rangle\\ &\quad -\frac{1}{2c}\varepsilon_{\mu\beta\gamma}R_{\beta}\omega i\langle\langle\hat{\mu}_{\lambda};\hat{\mu}_{\nu},\hat{\mu}_{\gamma}\rangle\rangle\\ &= -\frac{1}{2}|k|\varepsilon_{\nu\beta\gamma}R_{\beta}i\langle\langle\hat{\mu}_{\lambda};\hat{\mu}_{\mu},\hat{\mu}_{\gamma}\rangle\rangle\\ &\quad -\frac{1}{2}|k|\varepsilon_{\mu\beta\gamma}R_{\beta}i\langle\langle\hat{\mu}_{\lambda};\hat{\mu}_{\nu},\hat{\mu}_{\gamma}\rangle\rangle,\end{aligned} \tag{59}$$

where $|k'| = 2\omega/c$, and $|k| = \omega/c$. By using eqs. (58) and (59), one can prove, after expanding all the scalar molecular invariants present in eqs. (36)-(39), that:

$$a_{\mathbf{O}'} - a_{\mathbf{O}} = \langle\beta\Delta({}^{\beta}J)\rangle_a + |k|\langle\beta\Delta({}^{\beta}K)\rangle_a = 0, \tag{60}$$

$$b_{\mathbf{O}'} - b_{\mathbf{O}} = \langle\beta\Delta({}^{\alpha}J)\rangle_b + |k'|\langle\beta\Delta({}^{\alpha}K)\rangle_b = 0, \tag{61}$$

$$c_{\mathbf{O}'} - c_{\mathbf{O}} = \langle\beta\Delta({}^{\beta}J)\rangle_c + |k|\langle\beta\Delta({}^{\beta}K)\rangle_c = 0, \tag{62}$$

$$d_{\mathbf{O}'} - d_{\mathbf{O}} = |k'|\langle\beta\Delta({}^{\alpha}K)\rangle_d = 0, \tag{63}$$

where the symbol $\langle\beta\Delta({}^{\beta}J)\rangle_a$ signifies that the sum of all the scalar molecular invariants deriving from the gauge-origin shifts on the ${}^{\beta}J_{\lambda\mu\nu}$ tensor appearing in the a term, and similarly for the other symbols.
Consequently, the expressions for the a, b, c, and d terms of HRS-OA obtained at two different gauge origins **O** and **O′** are identical for exact wavefunctions, thus proving the origin-independence of the theory (i.e., there is not dependence on vector **R** when the gauge origin is $\mathbf{O}' = \mathbf{O} + \mathbf{R}$).

III. APPLICATIONS

A. Computational details

The ground state geometries of *R*-methyloxirane has been optimized using Gaussian16 (version RevA.03)[76] using Density Functional Theory (DFT) and in particular by employing the CAM-B3LYP range-separated hybrid functional[77] and the 6-311G(d,p) basis set (the Cartesian coordinates of the optimized geometry are provided in the Supporting Information file). To ensure the nature of the stationary state, a vibrational frequency calculation at the optimized geometry has been performed (all frequencies are positive). The *S* enantiomer of methyloxirane has been obtained from the optimized geometry of *R*-methyloxirane by the inversion operation ($\hat{i}$).
The molecular tensors in eqs. (9)-(13) have been obtained from the quadratic-response functions calculated at the TD-DFT level[78] with the functional CAM-B3LYP and using the quantum chemistry software DALTON (version 2020.0)[79]. In particular, the electric-dipole moment, the magnetic-dipole moment, and the traceless electric-quadrupole integrals have been computed using the `DIPLEN`, `ANGMOM`, and `THETA` keywords, respectively. The relationships between the actual operators in eqs. (21)-(23) and these keywords are[25]:

$$\hat{\mu}_{\alpha} = -1\cdot\alpha\texttt{DIPLEN} \tag{64}$$

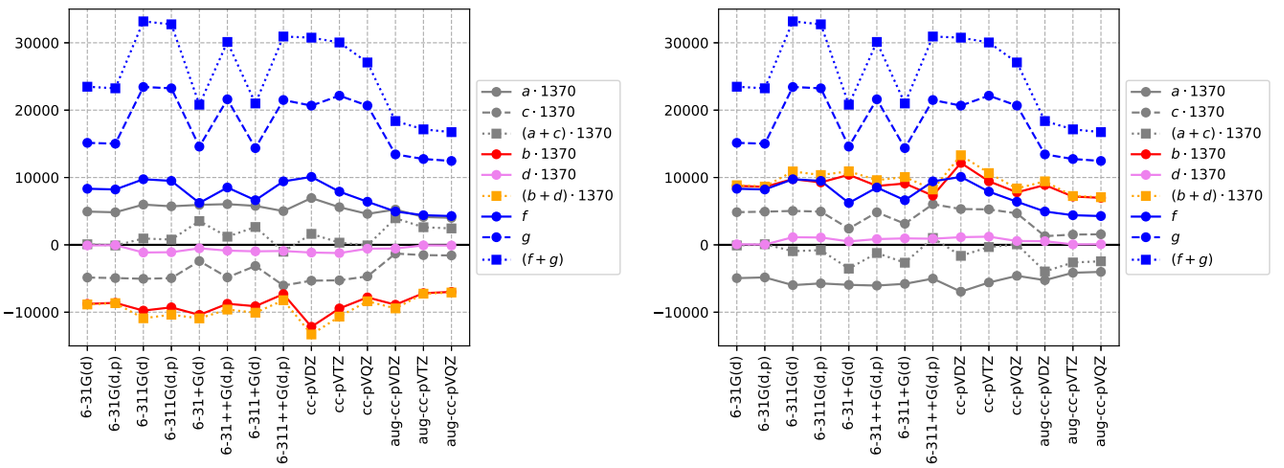

FIG. 3: The basis set dependence on the a, b, c, d, f and g terms of HRS-OA calculations for R- (left side) and S-methyloxirane (right side).

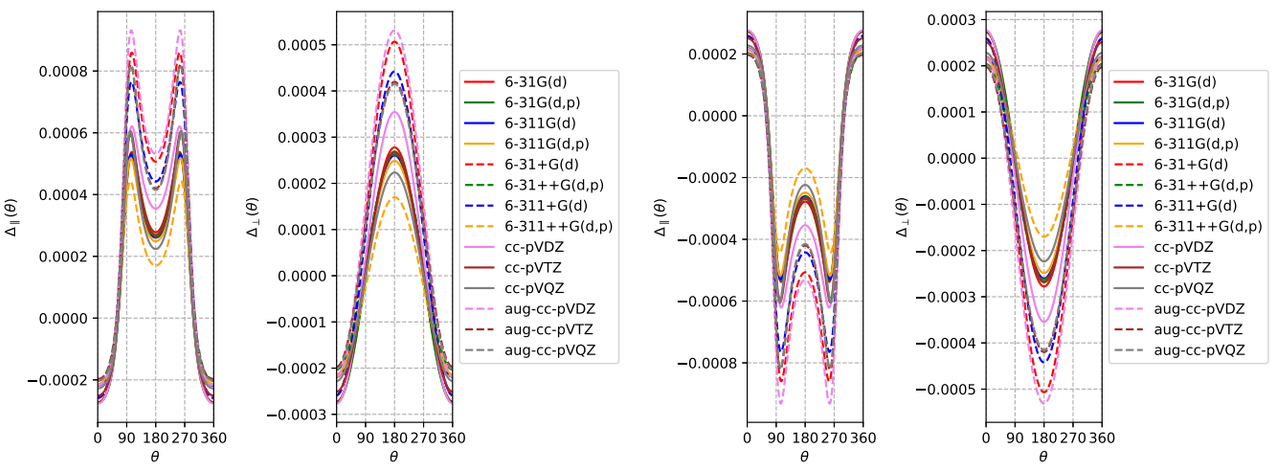

FIG. 4: The basis set dependence of the differential scattering ratios, $\Delta_{\parallel}(\theta)$ and $\Delta_{\perp}(\theta)$, for R- (left side) and S-methyloxirane (right side).

$$\hat{m}_{\alpha} = \frac{i}{2c} \cdot \alpha\texttt{ANGMOM} \tag{65}$$

$$\hat{Q}_{\alpha\beta} = -\frac{1}{3} \cdot \alpha\beta\texttt{THETA} \tag{66}$$

where α, β are generic indices belonging to the molecular frame (x, y, z). In eqs. (64) and (66) the -1 is due to the charge of the electron while in eq. (65) the factor $i/(2c)$ is due to the definition of the magnetic-dipole moment, see eq. (22). Consequently, the quadratic response function for the tensor $\beta_{\alpha\beta\gamma}$ is obtained as the opposite of the quadratic response function obtained from DALTON. At this point, the tensor $\beta_{\alpha\beta\gamma}$ is computed by using eq. (16) and by using the $1/2$ multiplication factor in eq. (15). The quadratic response functions for the tensors ${}^{\alpha}J_{\alpha\beta\gamma}$, and ${}^{\beta}J_{\alpha\beta\gamma}$ are obtained as $(i/2c)$ times the corresponding value obtained from DALTON. At this point, the tensors ${}^{\alpha}J_{\alpha\beta\gamma}$ and ${}^{\beta}J_{\alpha\beta\gamma}$ are computed by using eq. (17) and (18), respectively, and by applying the $1/2$ factor present in eq. (15). The quadratic response functions for the tensors ${}^{\alpha}K_{\alpha\beta\gamma\delta}$, and ${}^{\beta}K_{\alpha\beta\gamma\delta}$ are obtained as $-1/3$ times the corresponding value obtained from DALTON. This $1/3$ factor is due to the fact that the traceless electric-quadrupole operator is the one defined by Buckingham[80] which is three-times larger than the one defined in eq. (23) which is the one usually adopted in QED[66]. At this point, the tensors ${}^{\alpha}K_{\alpha\beta\gamma\delta}$ and ${}^{\beta}K_{\alpha\beta\gamma\delta}$ are computed by using eq. (19) and (20), respectively, and by applying the $1/2$ factor present in eq. (15). All transformations from the molecular tensor components to the macroscopic rotational-averaged quantities were performed with a homemade code.

TABLE I: The effect of different basis sets on terms a, b, c, d, f, and g for *R*-methyloxirane. Values are in atomic units (DFT, CAM-B3LYP).

Basis set	a	b	c	d	f	g
O						
6-31G(d)	3.61	-6.40	-3.54	-0.06	8331.89	15147.14
6-31G(d,p)	3.53	-6.29	-3.60	-0.03	8223.98	15020.68
6-311G(d)	4.36	-7.13	-3.68	-0.83	9742.41	23439.79
6-311G(d,p)	4.18	-6.77	-3.61	-0.80	9496.48	23246.10
6-31+G(d)	4.33	-7.59	-1.76	-0.38	6221.70	14588.00
6-31++G(d,p)	4.41	-6.39	-3.53	-0.63	8514.55	21608.51
6-311+G(d)	4.22	-6.65	-2.29	-0.70	6628.59	14365.32
6-311++G(d,p)	3.66	-5.34	-4.40	-0.66	9426.20	21505.08
cc-pVDZ	5.07	-8.88	-3.88	-0.83	10091.73	20670.94
cc-pVTZ	4.08	-6.89	-3.84	-0.89	7900.53	22149.49
cc-pVQZ	3.36	-5.69	-3.41	-0.42	6400.20	20676.59
aug-cc-pVDZ	3.83	-6.49	-0.94	-0.40	4950.79	13431.49
aug-cc-pVTZ	3.02	-5.24	-1.11	-0.05	4401.12	12746.97
aug-cc-pVQZ	2.93	-5.10	-1.15	-0.07	4276.95	12459.75
$\mathbf{O} \rightarrow \mathbf{O}' = \mathbf{O} + \mathbf{R}$						
6-31G(d)	3.55	-3.81	-8.68	-0.20	8331.89	15147.14
6-31G(d,p)	3.80	-3.34	-8.30	-0.17	8223.98	15020.68
6-311G(d)	8.92	2.56	-33.59	-1.03	9742.41	23439.79
6-311G(d,p)	9.10	2.80	-27.83	-1.01	9496.48	23246.10
6-31+G(d)	3.39	-19.45	-22.50	-0.64	6221.70	14588.00
6-31++G(d,p)	6.12	-16.65	-23.49	-1.00	8514.55	21608.51
6-311+G(d)	0.92	-8.92	-17.47	-0.97	6628.59	14365.32
6-311++G(d,p)	5.35	-14.55	-12.04	-1.05	9426.20	21505.08
cc-pVDZ	4.71	2.35	-17.47	-1.02	10091.73	20670.94
cc-pVTZ	6.12	3.98	-17.89	-1.09	7900.53	22149.49
cc-pVQZ	3.72	3.05	-12.94	-0.66	6400.20	20676.59
aug-cc-pVDZ	0.93	-5.73	2.80	-0.67	4950.79	13431.49
aug-cc-pVTZ	1.93	-4.35	-0.39	-0.31	4401.12	12746.97
aug-cc-pVQZ	2.41	-4.94	-0.51	-0.32	4276.95	12459.75
$\mathbf{O} \rightarrow \mathbf{O}' = \mathbf{O} + \mathbf{R}$ + *correction*						
6-31G(d)	3.62	-6.35	-3.53	-0.20	8331.89	15147.14
6-31G(d,p)	3.55	-6.23	-3.58	-0.17	8223.98	15020.68
6-311G(d)	4.39	-7.00	-3.63	-1.03	9742.41	23439.79
6-311G(d,p)	4.20	-6.68	-3.56	-1.01	9496.48	23246.10
6-31+G(d)	4.34	-7.47	-1.78	-0.64	6221.70	14588.00
6-31++G(d,p)	4.42	-6.18	-3.55	-1.00	8514.55	21608.51
6-311+G(d)	4.22	-6.45	-2.31	-0.97	6628.59	14365.32
6-311++G(d,p)	3.66	-5.09	-4.43	-1.05	9426.20	21505.08
cc-pVDZ	5.09	-8.77	-3.85	-1.02	10091.73	20670.94
cc-pVTZ	4.10	-6.89	-3.81	-1.09	7900.53	22149.49
cc-pVQZ	3.37	-5.58	-3.40	-0.66	6400.20	20676.59
aug-cc-pVDZ	3.83	-6.28	-0.97	-0.67	4950.79	13431.49
aug-cc-pVTZ	3.03	-5.16	-1.14	-0.31	4401.12	12746.97
aug-cc-pVQZ	2.93	-5.04	-1.17	-0.32	4276.95	12459.75

B. (*R*,*S*)-methyloxirane

1. *The basis set convergence*

The basis set convergence of the HRS-OA quantities was assessed by considering methyloxirane. We analyzed the performances of two basis set families: the Poples's and the Dunning's basis sets[81,82]. In particular, for both families, we considered basis functions with different degrees of polarization and with or without diffuse functions on heavy and eventually on hydrogen atoms. The basis set effects on the a, b, c, d, f and g terms of eqs. (34)-(41) are presented in Figure 3 and Figure 4 and, only for *R*-methyloxirane, in Table I. Note that these terms are quadratic quantities so that the variations as a function of the basis set size are naturally exalted with re-

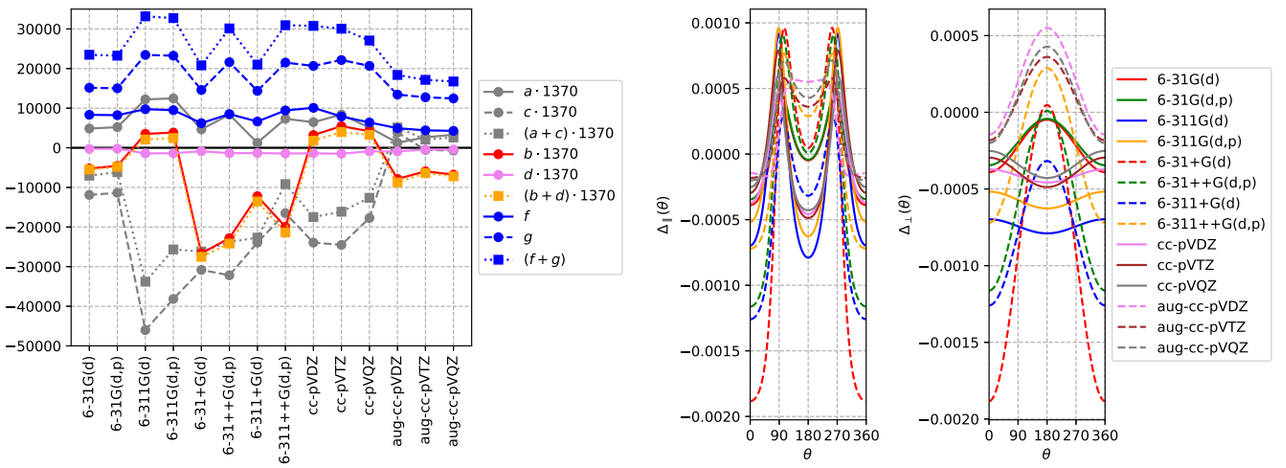

FIG. 5: The effect of changing the gauge-origin on the a, b, c, d, f, and g terms of HRS-OA differential scattering ration and their effect on $\Delta_\parallel(\theta)$ and $\Delta_\perp(\theta)$, for *R*-methyloxirane.

spect to what should be observed, for instance, for the β_{HRS} values[83]. In Figure 3 one can notice that the Pople's basis sets provide poorly converged results on all terms and especially on f and g terms. In particular, the use of basis sets with triple-ζ quality dramatically changes the value of the g term. Moreover, the presence of diffuse functions on hydrogen atoms seems to have important effects on f and g terms. On the other hand, Dunning's basis sets show an improved convergence. For aug-cc-pVXZ, with X = T, Q, the convergence is reached on a, b, c, d, f and g terms (variations of 5% or less).

A rather surprising fact from Figure 3 is that the basis set dependence of f (Eq. (40)) and g (Eq. (41)) terms do not follow the same trend, even if they contain only the scalar molecular invariants of $I(\langle\beta^2\rangle)$: g is more sensitive than f on the basis set quality. Moreover, f is always smaller than g. Also a and c terms do not follow the same basis set trends even if they contain the same kind of molecular invariants (except for the prefactors in front of them). Moreover, $|c|$ seems to be always smaller than $|a|$. Another interesting feature is the fact that c and a can have opposite signs (for a given basis set). For this reason we decided to plot also the basis set dependences for $(a+c)$ as well as $(f+g)$ which appear in the expression of $\Delta_\perp(\theta)$, see eq. (35).

From Table I one can notice that the "chiral" terms a, b, c, and d are 3 orders of magnitude smaller then the achiral and dominant terms f and g. Finally, for all basis sets, one can notice that f and g terms do not change ongoing from *R*-methyloxirane to *S*-methyloxirane, they are always positive. In fact, these terms contain the scalar molecular invariants of $I(\langle\beta^2\rangle)$ which are independent of the handness of the incident photons and represents the leading contribution to the total scattered intensity. On the other hand, a, b, c, and d terms change their signs ongoing from *R*-methyloxirane to *S*-methyloxirane. This mirror-image behaviour is more evident by looking at the differential scattering ratios, $\Delta_\parallel$ and $\Delta_\perp$, computed using eqs. (34) and (35), respectively, see Figure 4.

In Figure 4 one can see the final effect on the computed differential scattering ratios, $\Delta_\parallel$ and $\Delta_\perp$, as a function of the scattering angle θ. In particular, one can notice that the two enantiomers of methyloxirane give circular differential scattering ratios, which are mirror-images of each other. In particular, by looking at $\theta = 90°$, one can notice that the *R*-methyloxirane and *S*-methyloxirane give positive and negative differential scattering ratios, respectively. This shows how HRS-OA can be used to distinguish between enantiomers based on the sign obtained for $\Delta_\parallel$ or $\Delta_\perp$ at a particular scattering angle θ.

2. *The scattering angle and the experimental set-up*

An important feature that can be observed from Figure 4 is that the $\Delta_\parallel$ as a functions of the scattering angle θ behave almost like a "step" function around $\theta \approx \pm 90°$ (as an inflection point of the function $\Delta_\parallel(\theta)$). It seems that this scattering angle is an unstable region for $\Delta_\parallel$. From an experimental point of view, this means that, for perpendicular scattering angle configurations ($\theta = \pm 90°$), the HRS-OA measurements could potentially suffer from imprecision due to the geometrical incertitude of the experimental set-up.

3. *The origin dependence*

As said in Section II D, computations of mixed electric-magnetic properties suffer from the gauge-origin dependence issue when finite basis sets are employed. This limit can be resolved by using London atomic-orbitals (GIAO). Unfortunately, at present, the use of London atomic orbitals is not available in the Dalton software for the targeted quadratic response functions. Moreover, the electric quadrupole moment is origin-independent if the net charge and the electric-dipole moment of the system are both zero[69]. Consequently, for

methyloxirane, which is a neutral and polar molecule, also the ${}^{\alpha}K_{\alpha\beta\gamma\delta}$ and ${}^{\beta}K_{\alpha\beta\gamma\delta}$ mixed first hyperpolarizabilities are origin-dependent.

We analyzed the origin-dependence of our computations by moving the COM of the system to an arbitrary position by using the vector $\mathbf{R}_{\text{mol}} = (9.5415, -18.9691, 28.3372)$ a.u., which is large compared to the molecule size. The gauge origin changes by a vector $\mathbf{R} = -\mathbf{R}_{\text{mol}}$. The impact of the change of gauge origin is visualized in Figure 5 and in Table I. First, as expected, the pure-electric first hyperpolarizability is origin-independent. On the other hand, the effect on the mixed electric-magnetic dipole hyperpolarizabilities is important and persist for all basis sets. This origin-dependence is however attenuated for the aug-cc-VTXZ with X = T, Q, basis set, see Figure S2 and Table S3 in the SI file.

A possible artificial strategy to remove the effect of displacing the COM of the molecule in space (origin-dependence) is represented by subtracting the $\Delta({}^{\alpha}J_{\lambda\mu\nu})$, $\Delta({}^{\beta}J_{\lambda\mu\nu})$, $\Delta({}^{\alpha}K_{\lambda\mu\nu o})$, and $\Delta({}^{\beta}K_{\lambda\mu\nu o})$ shifts from eqs. (46), (48), (51), and (53) respectively. This comparison between the two sets of data also substantiates the validity of the derivations of eqs. (46)-(54). For example, to restore the HRS-OA values obtained for the molecule whose COM is placed at the origin (Table I on top), these shifts in ${}^{\alpha}J_{\lambda\mu\nu}$, ${}^{\beta}J_{\lambda\mu\nu}$, ${}^{\alpha}K_{\lambda\mu\nu o}$, and ${}^{\beta}K_{\lambda\mu\nu o}$ tensors, eqs. (47), (49), (52) and (54) were subtracted from eqs. (46), (48), (51), and (53) respectively. The results for the a, b, c, d, f and g terms are presented in Table I. It is clear that the effects of the displacement of the COM can be removed from the a, b and c terms.

IV. CONCLUSIONS

The phenomenon of HRS-OA, whose theory was first formulated by Andrews and Thirunamchandran[28], and recently exhibited in a series of experimental studies by different groups[31–34], has been reviewed in view of a first quantum chemical investigation. We re-derived the necessary equations for the simulation of HRS-OA experiments and proved the origin-independence of the theory for exact wavefunctions. For the first time, this enabled the simulation of HRS-OA experiments at the TD-DFT level. Our computations show that HRS-OA can be used to distinguish between the enantiomers of the same molecule because the signals from two enantiomers are mirror-images.

The basis set analysis on the HRS-OA of the prototypical methyloxirane compound shows important basis set dependence, especially for Pople's basis sets. The convergence is reached only by using Dunning's basis sets with diffused and polarization functions, i.e., for aug-cc-pVXZ, with X = T, Q. This requirement of large basis sets for converged results is quite common for nonlinear electric-magnetic properties. By using finite basis sets, our results are origin-dependent. This could be an issue for reliable computations of HRS-OA and comparison with experiments and a solution to it should be considered in future works. One possible strategy that can be followed is the above mentioned use of London atomic-orbitals (GIAO). In future works, we plan to extend our computational implementation of HRS-OA to other chiral molecules, as well other types of chiral light. In particular, it has recently been highlighted[54] how future HRS-OA experiments may benefit from exploiting an additional degree of optical chirality present in optical vortex beams which carry orbital angular momentum.

SUPPLEMENTARY MATERIAL

The rotational averaging procedure, required for finding the final expressions for the circular differential scattering ratios, eqs. (34)-(41), and the effect of the origin-dependence with the basis-set size are provided as the supplementary material.

ACKNOWLEDGMENTS

A. B. and B. C. would like to thank F.R.S. - FNRS (Nonlinear chiroptics project) GRANT n° T.0025.22. A. B. and B. C. would like to thank Prof. Vincent Rodriguez for helpful discussions on HRS-OA.

DATA AVAILABILITY STATEMENT

The data that support the findings of this study are available within the article and its supplementary material.

[1] R. S. Cahn, C. Ingold, and V. Prelog, "Specification of Molecular Chirality," Angew. Chemie Int. Ed. English **5**, 385–415 (1966).
[2] F. A. Cotton, *Chemical Applications of Group Theory* (Wiley, New York, NY, 1990) pp. 1–461.
[3] D. M. Bishop, *Group Theory and Chemistry* (Dover, Oxford, England, 1993) pp. 1–300.
[4] G. H. Wagnière, *Chirality Univers. Asymmetry Reflections Image Mirror Image* (Wiley, Zürich, 2008) pp. 1–247.
[5] A. Guijarro and M. Yus, *Orig. Chirality Mol. Life* (Royal Society of Chemistry, Cambridge, 2008) pp. 1–150.
[6] J. S. Richardson, "The Anatomy and Taxonomy of Protein Structure," in *Adv. Protein Chem.*, Vol. 34 (Academic Press, New York, NY, 1981) pp. 167–339.
[7] R. E. Dickerson, H. R. Drew, B. N. Conner, R. M. Wing, A. V. Fratini, and M. L. Kopka, "The anatomy of A-, B-, and Z-DNA," Science (80-.). **216**, 475–485 (1982).
[8] W. L. Bragg, D. C. Phillips, and H. F. Lipson, *The Development of X-ray Analysis* (Hafner Press, London, UK, 1975) pp. 1–270.
[9] T. J. Wenzel and J. D. Wilcox, "Chiral reagents for the determination of enantiomeric excess and absolute configuration using NMR spectroscopy," Chirality **15**, 256–270 (2003).
[10] N. Berova, P. L. Polavarapu, K. Nakanishi, and R. W. Woody, *Compr. Chiroptical Spectrosc. Instrumentation, Methodol. Theor. Simulations*, edited by N. Berova, P. L. Polavarapu, K. Nakanishi, and R. W. Woody, Vol. 1 (John Wiley & Sons, Inc., Hoboken, NJ, USA, 2011) pp. 1–791.
[11] M. Klessinger and J. Michl, *Excited States and Photochemistry of Organic Molecules* (Wiley-VCH, Cambridge, UK, 1995) pp. 1–564.
[12] P. H. Vaccaro, "Optical rotation and intrinsic optical activity," in *Compr. Chiroptical Spectrosc. Instrumentation, Methodol. Theor. Simulations* (John Wiley & Sons, Inc., Hoboken, NJ, USA, 2011) pp. 275–323.
[13] N. Berova, K. Nakanishi, and R. W. Woody, *Circular Dichroism: Principles and Applications, 2nd Edition*, Vol. 367 (Wiley-VCH, New York, NY, 2000) pp. 1–878.
[14] I. Warnke and F. Furche, "Circular dichroism: Electronic," Wiley Interdiscip. Rev. Comput. Mol. Sci. **2**, 150–166 (2012).

[15]J. P. Riehl and G. Muller, "Circularly polarized luminescence spectroscopy and emission-detected circular dichroism," in *Compr. Chiroptical Spectrosc. Instrumentation, Methodol. Theor. Simulations* (John Wiley & Sons, Inc., Hoboken, NJ, USA, 2011) pp. 65–90.
[16]S. Abbate, E. Castiglioni, F. Gangemi, R. Gangemi, and G. Longhi, "NIR-VCD, vibrational circular dichroism in the near-infrared: Experiments, theory and calculations," Chirality **21**, E242–E252 (2009).
[17]L. D. Barron, F. Zhu, L. Hecht, G. E. Tranter, and N. W. Isaacs, "Raman optical activity: An incisive probe of molecular chirality and biomolecular structure," J. Mol. Struct. **834-836**, 7–16 (2007).
[18]G. Pescitelli, L. Di Bari, and N. Berova, "Application of electronic circular dichroism in the study of supramolecular systems," Chem. Soc. Rev. **43**, 5211–5233 (2014).
[19]Y. R. Shen, *The Principles of Nonlinear Optics*, Wiley classics library (Wiley, New York, NY, 1984) pp. 1–563.
[20]R. W. Boyd, *Nonlinear Optics*, third edit ed. (Academic Press, Burlington, 2008) pp. 1–613.
[21]I. Tinoco, "Two-photon circular dichroism," J. Chem. Phys. **62**, 1006–1009 (1975).
[22]E. A. Power, "Two-photon circular dichroism," J. Chem. Phys. **63**, 1348–1350 (1975).
[23]C. Toro, L. De Boni, N. Lin, F. Santoro, A. Rizzo, and F. E. Hernandez, "Two-Photon Absorption Circular Dichroism: A New Twist in Nonlinear Spectroscopy," Chem. - A Eur. J. **16**, 3504–3509 (2010).
[24]F. E. Hernández and A. Rizzo, "Two-Photon Polarization Dependent Spectroscopy in Chirality: A Novel Experimental-Theoretical Approach to Study Optically Active Systems," Molecules **16**, 3315–3337 (2011).
[25]D. H. Friese and K. Ruud, "Three-photon circular dichroism: towards a generalization of chiroptical non-linear light absorption," Phys. Chem. Chem. Phys. **18**, 4174–4184 (2016).
[26]N. Ji and Y. R. Shen, "A novel spectroscopic probe for molecular chirality," Chirality **18**, 146–158 (2006).
[27]V. K. Valev, "Characterization of Nanostructured Plasmonic Surfaces with Second Harmonic Generation," Langmuir **28**, 15454–15471 (2012).
[28]D. L. Andrews and T. Thirunamachandran, "Hyper-Raman scattering by chiral molecules," J. Chem. Phys. **70**, 1027 (1979).
[29]D. L. Andrews and T. Thirunamachandran, "The hyper-Raman effect: A new approach to vibrational mode classification and assignment of spectral lines," J. Chem. Phys. **68**, 2941 (1978).
[30]T. Verbiest, K. Clays, and V. Rodriguez, *Second. Nonlinear Opt. Charact. Tech.* (CRC Press, Boca Raton, 2009) pp. 1–192.
[31]J. T. Collins, K. R. Rusimova, D. C. Hooper, H.-H. Jeong, L. Ohnoutek, F. Pradaux-Caggiano, T. Verbiest, D. R. Carbery, P. Fischer, and V. K. Valev, "First Observation of Optical Activity in Hyper-Rayleigh Scattering," Phys. Rev. X **9**, 011024 (2019).
[32]L. Ohnoutek, N. H. Cho, A. W. Allen Murphy, H. Kim, D. M. Răsădean, G. D. Pantoş, K. T. Nam, and V. K. Valev, "Single Nanoparticle Chiroptics in a Liquid: Optical Activity in Hyper-Rayleigh Scattering from Au Helicoids," Nano Lett. **20**, 5792–5798 (2020).
[33]L. Ohnoutek, B. J. Olohan, R. R. Jones, X. Zheng, H. H. Jeong, and V. K. Valev, "Second harmonic Rayleigh scattering optical activity of single Ag nanohelices in a liquid," Nanoscale **14**, 3888–3898 (2022).
[34]D. Verreault, K. Moreno, É. Merlet, F. Adamietz, B. Kauffmann, Y. Ferrand, C. Olivier, and V. Rodriguez, "Hyper-Rayleigh Scattering as a New Chiroptical Method: Uncovering the Nonlinear Optical Activity of Aromatic Oligoamide Foldamers," J. Am. Chem. Soc. **142**, 257–263 (2020).
[35]J. S. Ford and D. L. Andrews, "Molecular Tensor Analysis of Third-Harmonic Scattering in Liquids," J. Phys. Chem. A **122**, 563–573 (2018).
[36]D. L. Andrews, "Irreducible Cartesian Tensor Analysis of Harmonic Scattering from Chiral Fluids," Symmetry (Basel). **12**, 1466 (2020).
[37]L. Ohnoutek, H. Jeong, R. R. Jones, J. Sachs, B. J. Olohan, D. Răsădean, G. D. Pantoş, D. L. Andrews, P. Fischer, and V. K. Valev, "Optical Activity in Third-Harmonic Rayleigh Scattering: A New Route for Measuring Chirality," Laser Photon. Rev. **15**, 2100235 (2021).
[38]F. Furche, R. Ahlrichs, C. Wachsmann, E. Weber, A. Sobanski, F. Vögtle, and S. Grimme, "Circular dichroism of helicenes investigated by time-dependent density functional theory," J. Am. Chem. Soc. **122**, 1717–1724 (2000).
[39]B. Jansík, A. Rizzo, H. Ågren, and B. Champagne, "Strong two-photon circular dichroism in helicenes: A theoretical investigation," J. Chem. Theory Comput. **4**, 457–467 (2008).
[40]M. Pecul and K. Ruud, "The Ab Initio Calculation of Optical Rotation and Electronic Circular Dichroism," in *Adv. Quantum Chem.*, Vol. 50 (Elsevier Academic Press, Amsterdam, 2005) pp. 185–212.
[41]R. D'Cunha and T. D. Crawford, "Modeling Complex Solvent Effects on the Optical Rotation of Chiral Molecules: A Combined Molecular Dynamics and Density Functional Theory Study," J. Phys. Chem. A **125**, 3095–3108 (2021).
[42]G. Pescitelli, L. Di Bari, and N. Berova, "Conformational aspects in the studies of organic compounds by electronic circular dichroism," Chem. Soc. Rev. **40**, 4603–4625 (2011).
[43]C. Diaz, N. Lin, C. Toro, R. Passier, A. Rizzo, and F. E. Hernández, "The Effect of the π-Electron Delocalization Curvature on the Two-Photon Circular Dichroism of Molecules with Axial Chirality," J. Phys. Chem. Lett. **3**, 1808–1813 (2012).
[44]M. Srebro-Hooper and J. Autschbach, "Calculating Natural Optical Activity of Molecules from First Principles," Annu. Rev. Phys. Chem. **68**, 399–420 (2017).
[45]E. A. Power and S. Zienau, "Coulomb gauge in non-relativistic quantum electro-dynamics and the shape of spectral lines," Philos. Trans. R. Soc. London. Ser. A, Math. Phys. Sci. **251**, 427–454 (1959).
[46]R. G. Woolley, "Molecular quantum electrodynamics," Proc. R. Soc. London. A. Math. Phys. Sci. **321**, 557–572 (1971).
[47]D. Craig and T. Thirunamachandran, "Radiation–Molecule Interactions in Chemical Physics," in *Adv. Quantum Chem.*, Vol. 16 (1982) pp. 97–160.
[48]D. L. Andrews, D. P. Craig, and T. Thirunamachandran, "Molecular quantum electrodynamics in chemical physics," Int. Rev. Phys. Chem. **8**, 339–383 (1989).
[49]D. P. Craig and T. Thirunamachandran, *Molecular Quantum Electrodynamics: An Introduction to Radiation-molecule Interactions*, Dover Books on Chemistry Series (Dover Publications, Mineola, New York, 1998) pp. 1–324.
[50]D. L. Andrews, G. A. Jones, A. Salam, and R. G. Woolley, "Perspective: Quantum Hamiltonians for optical interactions," J. Chem. Phys. **148**, 040901 (2018), arXiv:1801.07735.
[51]D. L. Andrews, D. S. Bradshaw, K. A. Forbes, and A. Salam, "Quantum electrodynamics in modern optics and photonics: tutorial," J. Opt. Soc. Am. B **37**, 1153 (2020).
[52]D. S. Bradshaw, K. A. Forbes, and D. L. Andrews, "Quantum field representation of photon-molecule interactions," Eur. J. Phys. **41**, 025406 (2020).
[53]D. L. Andrews, "Quantum formulation for nanoscale optical and material chirality: symmetry issues, space and time parity, and observables," J. Opt. **20**, 033003 (2018).
[54]K. A. Forbes, "Nonlinear chiral molecular photonics using twisted light: hyper-Rayleigh and hyper-Raman optical activity," J. Opt. **22**, 095401 (2020).
[55]D. L. Andrews and P. Allcock, *Optical Harmonics in Molecular Systems* (Wiley, Weinheim, Germany, 2002) pp. 1–253.
[56]D. L. Andrews, "The role of longitudinal polarization in surface second harmonic generation," J. Mod. Opt. **40**, 931–938 (1993).
[57]D. L. Andrews, "Symmetries, conserved properties, tensor representations, and irreducible forms in molecular quantum electrodynamics," Symmetry (Basel). **10** (2018), 10.3390/sym10070298.
[58]J. Olsen and P. Jørgensen, "Linear and nonlinear response functions for an exact state and for an MCSCF state," J. Chem. Phys. **82**, 3235–3264 (1984).
[59]P. Norman and K. Ruud, "Microscopic Theory of Nonlinear Optics," in *Challenges Adv. Comput. Chem. Phys.*, Vol. 1 (Springer, Dordrecht, The Netherlands, 2006) pp. 1–49.
[60]M. Stähelin, C. R. Moylan, D. M. Burland, A. Willetts, J. E. Rice, D. P. Shelton, and E. A. Donley, "A comparison of calculated and experimental hyperpolarizabilities for acetonitrile in gas and liquid phases," J. Chem. Phys. **98**, 5595–5603 (1993).
[61]H. Reis, "Problems in the comparison of theoretical and experimental hyperpolarizabilities revisited," J. Chem. Phys. **125**, 014506 (2006).
[62]P. Norman, K. Ruud, and T. Saue, *Principles and practices of molecular properties: Theory, modeling and simulations* (John Wiley & Sons, Ltd, Chichester, UK, 2017) pp. 1–468.
[63]T. B. Pedersen, "Introduction to Response Theory," in *Handb. Comput. Chem.* (Springer International Publishing, Cham, 2017) pp. 269–294.

[64]M. Jaszuński, A. Rizzo, and K. Ruud, "Molecular electric, magnetic, and optical properties," in *Handb. Comput. Chem.* (Springer International Publishing, Cham, 2017) pp. 497–592.
[65]E. A. Power and T. Thirunamachandran, "Circular dichroism: A general theory based on quantum electrodynamics," J. Chem. Phys. **60**, 3695–3701 (1974).
[66]D. L. Andrews, "Rayleigh and Raman optical activity: An analysis of the dependence on scattering angle," J. Chem. Phys. **72**, 4141–4144 (1980).
[67]S. Coriani, M. Pecul, A. Rizzo, P. Jørgensen, and M. Jaszuński, "Ab initio study of magnetochiral birefringence," J. Chem. Phys. **117**, 6417–6428 (2002).
[68]J. Autschbach, "Ab initio electronic circular dichroism and optical rotatory dispersion: From organic molecules to transition metal complexes," in *Compr. Chiroptical Spectrosc. Instrumentation, Methodol. Theor. Simulations* (John Wiley & Sons, Inc., Hoboken, NJ, USA, 2011) pp. 593–642.
[69]L. D. Barron, *Molecular Light Scattering and Optical Activity* (Cambridge University Press, Cambridge, UK, 2004).
[70]D. L. Andrews and T. Thirunamachandran, "On three-dimensional rotational averages," J. Chem. Phys. **67**, 5026–5033 (1977).
[71]T. Helgaker and P. Jørgensen, "An electronic Hamiltonian for origin independent calculations of magnetic properties," J. Chem. Phys. **95**, 2595–2801 (1991).
[72]A. Rizzo and H. Ågren, "Ab initio study of the circular intensity difference in electric-field-induced second harmonic generation of chiral natural amino acids," Phys. Chem. Chem. Phys. **15**, 1198–1207 (2013).
[73]K. Ruud, T. Helgaker, K. L. Bak, P. Jørgensen, and H. J. A. Jensen, "Hartree-Fock limit magnetizabilities from London orbitals," J. Chem. Phys. **99**, 3847–3859 (1993).
[74]K. Ruud, T. Helgaker, R. Kobayashi, P. Jørgensen, K. L. Bak, and H. J. A. Jensen, "Multiconfigurational self-consistent field calculations of nuclear shieldings using London atomic orbitals," J. Chem. Phys. **100**, 8178–8185 (1994).
[75]J. Olsen and P. Jørgensen, "Time-Dependent Response Theory with Applications to Self-Consistent Field and Multiconfigurational Self-Consistent Field Wave Functions," in *Mod. Electron. Struct. Theory* (1995) pp. 857–990.
[76]M. J. Frisch, G. W. Trucks, H. B. Schlegel, G. E. Scuseria, M. A. Robb, J. R. Cheeseman, G. Scalmani, V. Barone, G. A. Petersson, H. Nakatsuji, X. Li, M. Caricato, A. V. Marenich, J. Bloino, B. G. Janesko, R. Gomperts, B. Mennucci, D. J. Hratch, M. J. Frisch, G. W. Trucks, H. B. Schlegel, G. E. Scuseria, M. A. Robb, J. R. Cheeseman, G. Scalmani, V. Barone, G. A. Petersson, H. Nakatsuji, X. Li, M. Caricato, A. V. Marenich, J. Bloino, B. G. Janesko, R. Gomperts, B. Mennucci, H. P. Hratchian, J. V. Ortiz, A. F. Izmaylov, J. L. Sonnenberg, D. Williams-Young, F. Ding, F. Lipparini, F. Egidi, J. Goings, B. Peng, A. Petrone, T. Henderson, D. Ranasinghe, V. G. Zakrzewski, J. Gao, N. Rega, G. Zheng, W. Liang, M. Hada, M. Ehara, K. Toyota, R. Fukuda, J. Hasegawa, M. Ishida, T. Nakajima, Y. Honda, O. Kitao, H. Nakai, T. Vreven, K. Throssell, J. A. Montgomery Jr., J. E. Peralta, F. Ogliaro, M. J. Bearpark, J. J. Heyd, E. N. Brothers, K. N. Kudin, V. N. Staroverov, T. A. Keith, R. Kobayashi, J. Normand, K. Raghavachari, A. P. Rendell, J. C. Burant, S. S. Iyengar, J. Tomasi, M. Cossi, J. M. Millam, M. Klene, C. Adamo, R. Cammi, J. W. Ochterski, R. L. Martin, K. Morokuma, O. Farkas, J. B. Foresman, and D. J. Fox, "Gaussian16 Revision C.01," (2016).
[77]T. Yanai, D. P. Tew, and N. C. Handy, "A new hybrid exchange–correlation functional using the Coulomb-attenuating method (CAM-B3LYP)," Chem. Phys. Lett. **393**, 51–57 (2004).
[78]T. Helgaker, S. Coriani, P. Jørgensen, K. Kristensen, J. Olsen, and K. Ruud, "Recent advances in wave function-based methods of molecular-property calculations," Chem. Rev. **112**, 543–631 (2012).
[79]K. Aidas, C. Angeli, K. L. Bak, V. Bakken, R. Bast, L. Boman, O. Christiansen, R. Cimiraglia, S. Coriani, P. Dahle, E. K. Dalskov, U. Ekström, T. Enevoldsen, J. J. Eriksen, P. Ettenhuber, B. Fernández, L. Ferrighi, H. Fliegl, L. Frediani, K. Hald, A. Halkier, C. Hättig, H. Heiberg, T. Helgaker, A. C. Hennum, H. Hettema, E. Hjertenæs, S. Høst, I. M. Høyvik, M. F. Iozzi, B. Jansík, H. J. A. Jensen, D. Jonsson, P. Jørgensen, J. Kauczor, S. Kirpekar, T. Kjærgaard, W. Klopper, S. Knecht, R. Kobayashi, H. Koch, J. Kongsted, A. Krapp, K. Kristensen, A. Ligabue, O. B. Lutnæs, J. I. Melo, K. V. Mikkelsen, R. H. Myhre, C. Neiss, C. B. Nielsen, P. Norman, J. Olsen, J. M. H. Olsen, A. Osted, M. J. Packer, F. Pawlowski, T. B. Pedersen, P. F. Provasi, S. Reine, Z. Rinkevicius, T. A. Ruden, K. Ruud, V. V. Rybkin, P. Sałek, C. C. Samson, A. S. de Merás, T. Saue, S. P. Sauer, B. Schimmelpfennig, K. Sneskov, A. H. Steindal, K. O. Sylvester-Hvid, P. R. Taylor, A. M. Teale, E. I. Tellgren, D. P. Tew, A. J. Thorvaldsen, L. Thøgersen, O. Vahtras, M. A. Watson, D. J. Wilson, M. Ziolkowski, and H. Ågren, "The Dalton quantum chemistry program system," Wiley Interdiscip. Rev. Comput. Mol. Sci. **4**, 269–284 (2014).
[80]A. D. Buckingham, "Permanent and Induced Molecular Moments and Long-Range Intermolecular Forces," in *Adv. Chem. Phys. Intermol. Forces, Vol. 12*, edited by Joseph O. Hirschfelder (John Wiley & Sons, Inc., 1967) pp. 107–142.
[81]R. Ditchfield, W. J. Hehre, and J. A. Pople, "Self-Consistent Molecular-Orbital Methods. IX. An Extended Gaussian-Type Basis for Molecular-Orbital Studies of Organic Molecules," J. Chem. Phys. **54**, 724–728 (1971).
[82]T. H. Dunning, "Gaussian basis sets for use in correlated molecular calculations. I. The atoms boron through neon and hydrogen," J. Chem. Phys. **90**, 1007–1023 (1989).
[83]F. Castet, E. Bogdan, A. Plaquet, L. Ducasse, B. Champagne, and V. Rodriguez, "Reference molecules for nonlinear optics: A joint experimental and theoretical investigation," J. Chem. Phys. **136**, 024506 (2012).

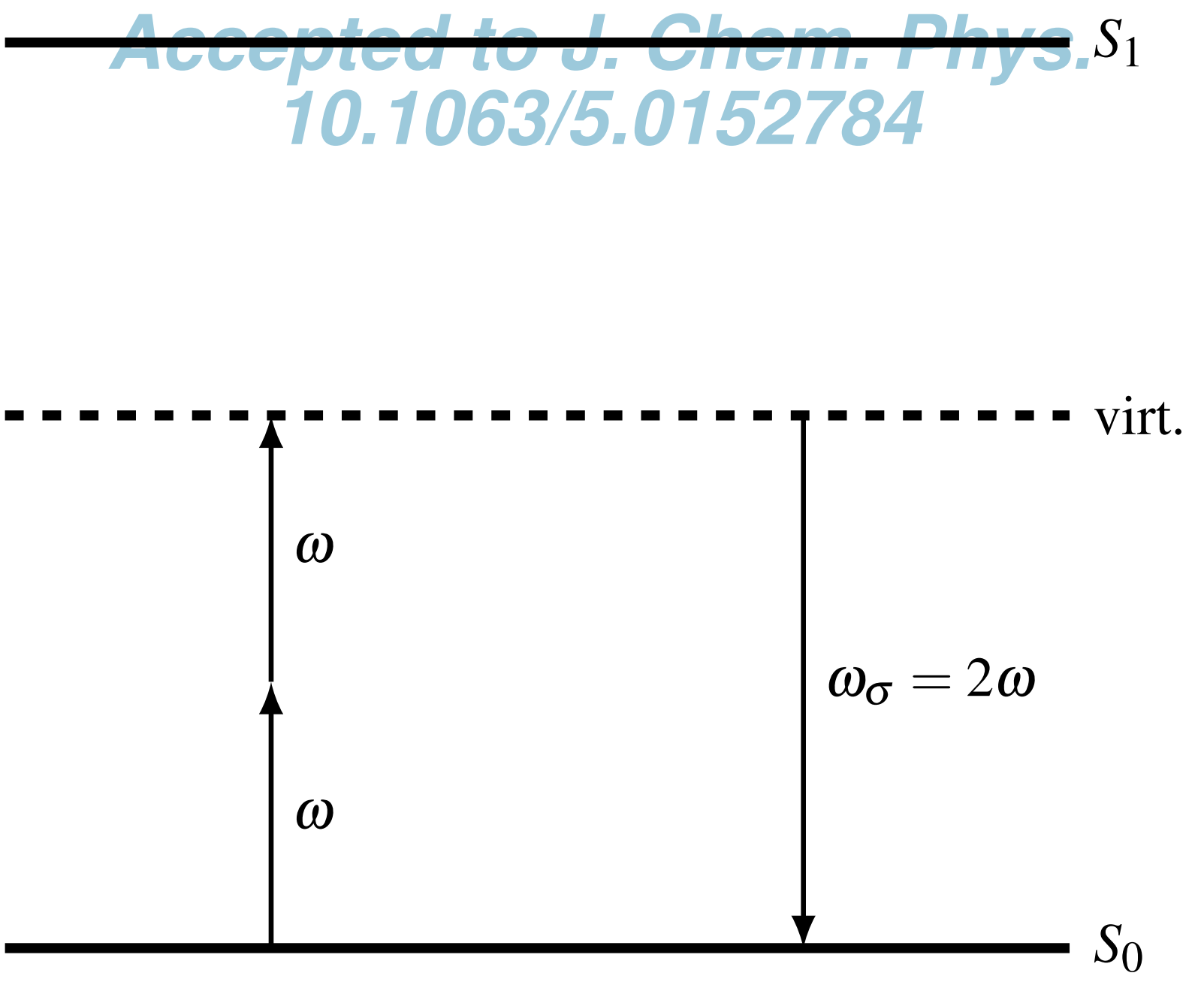

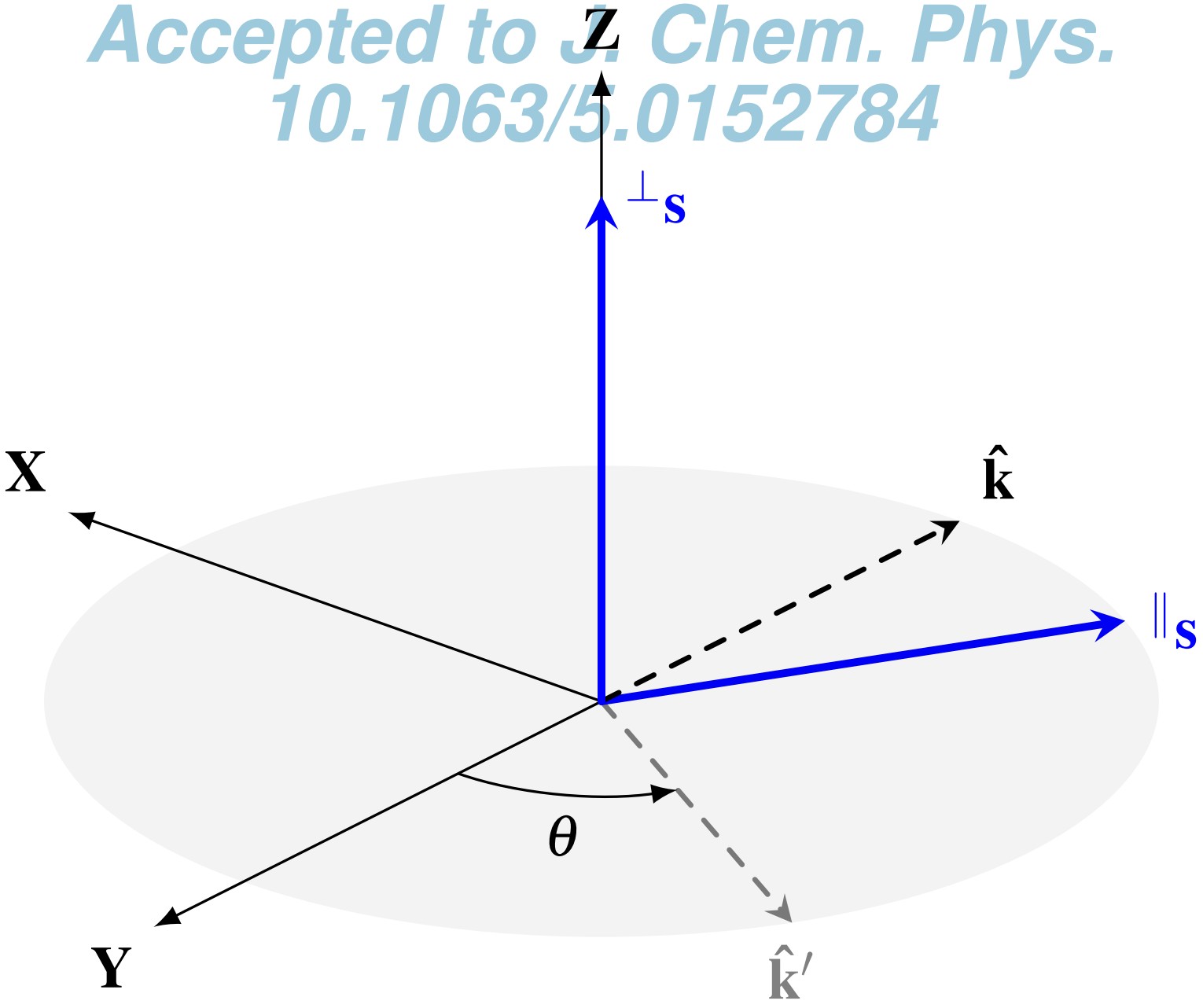

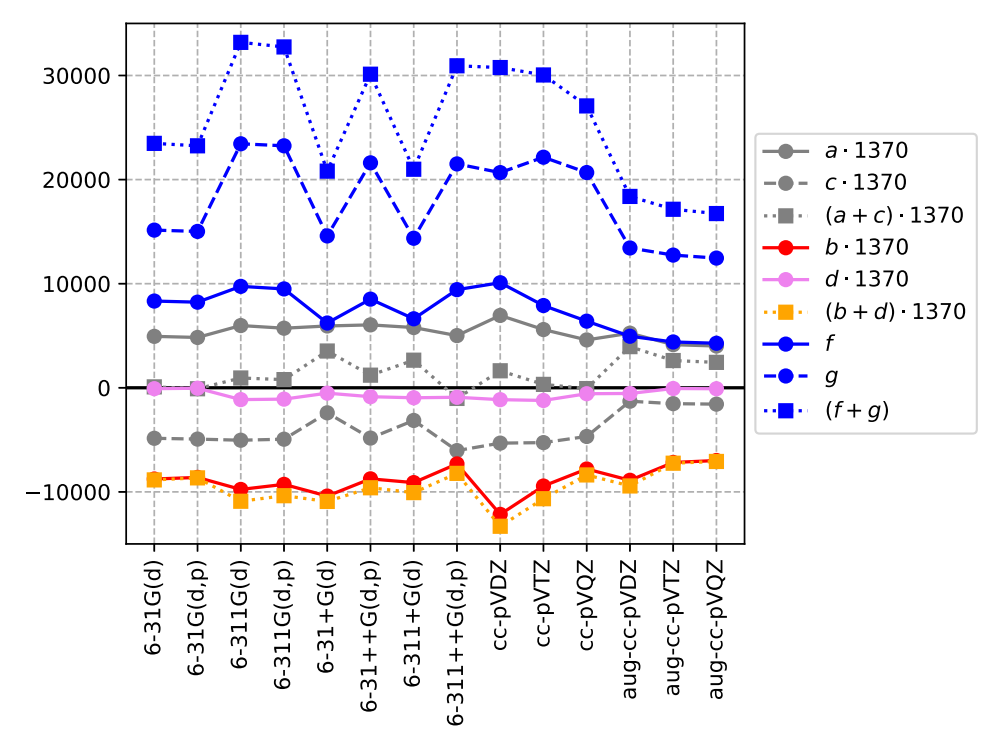
30000
20000
10000
0
−10000
6-31G(d)
6-31G(d,p)
6-311G(d)
6-311G(d,p)
6-31+G(d)
6-31++G(d,p)
6-311+G(d)
6-311++G(d,p)
cc-pVDZ
cc-pVTZ
cc-pVQZ
aug-cc-pVDZ
aug-cc-pVTZ
aug-cc-pVQZ
$a \cdot 1370$
$c \cdot 1370$
$(a+c) \cdot 1370$
$b \cdot 1370$
$d \cdot 1370$
$(b+d) \cdot 1370$
f
g
$(f+g)$

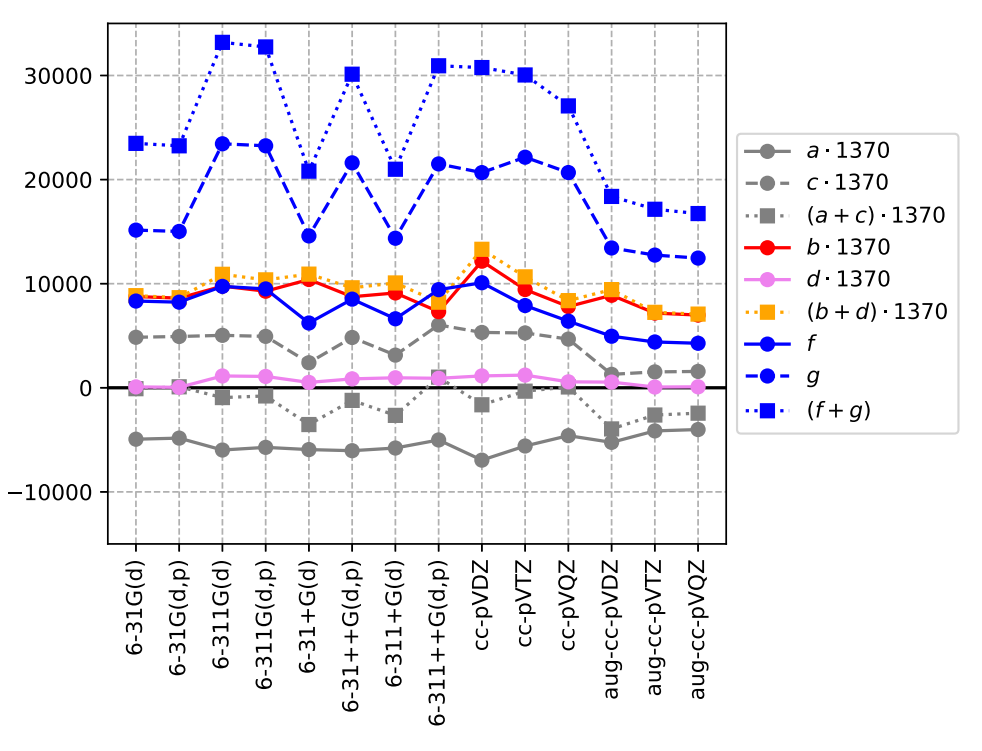
30000
20000
10000
0
−10000
6-31G(d)
6-31G(d,p)
6-311G(d)
6-311G(d,p)
6-31+G(d)
6-31++G(d,p)
6-311+G(d)
6-311++G(d,p)
cc-pVDZ
cc-pVTZ
cc-pVQZ
aug-cc-pVDZ
aug-cc-pVTZ
aug-cc-pVQZ
$a \cdot 1370$
$c \cdot 1370$
$(a+c) \cdot 1370$
$b \cdot 1370$
$d \cdot 1370$
$(b+d) \cdot 1370$
f
g
$(f+g)$

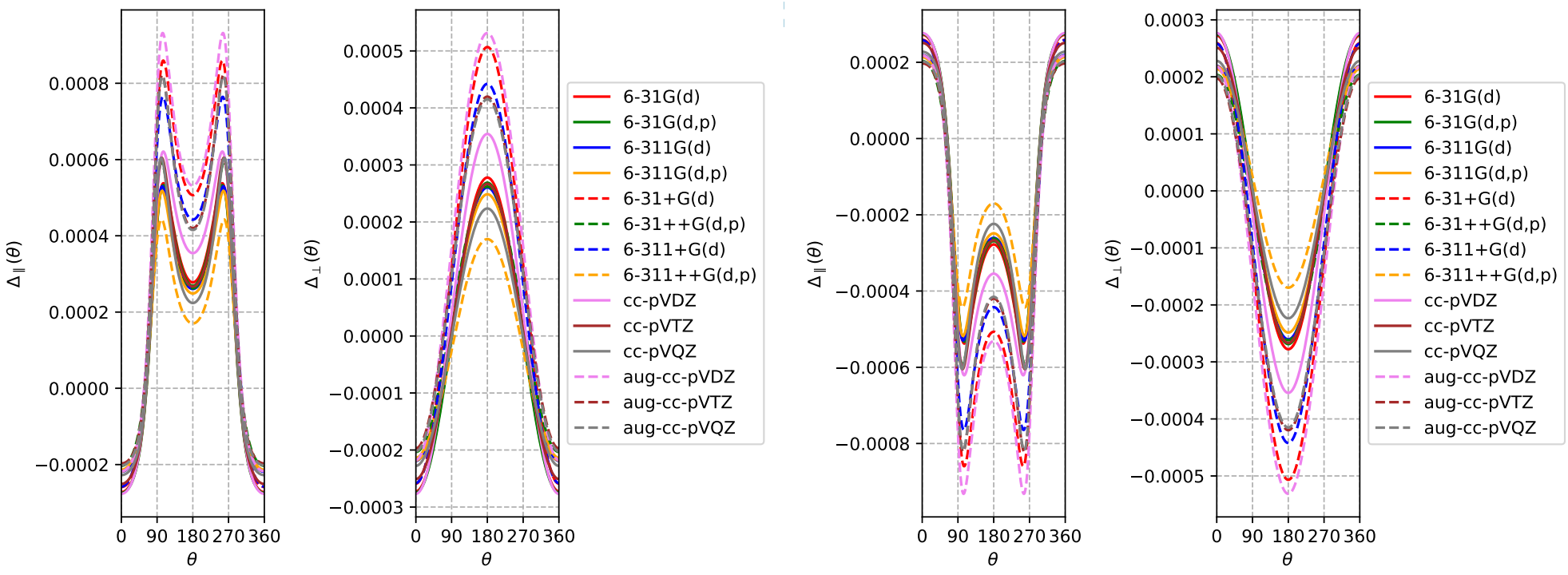
$\Delta_{\parallel}(\theta)$
$\Delta_{\perp}(\theta)$
θ
0 90 180 270 360
6-31G(d)
6-31G(d,p)
6-311G(d)
6-311G(d,p)
6-31+G(d)
6-31++G(d,p)
6-311+G(d)
6-311++G(d,p)
cc-pVDZ
cc-pVTZ
cc-pVQZ
aug-cc-pVDZ
aug-cc-pVTZ
aug-cc-pVQZ

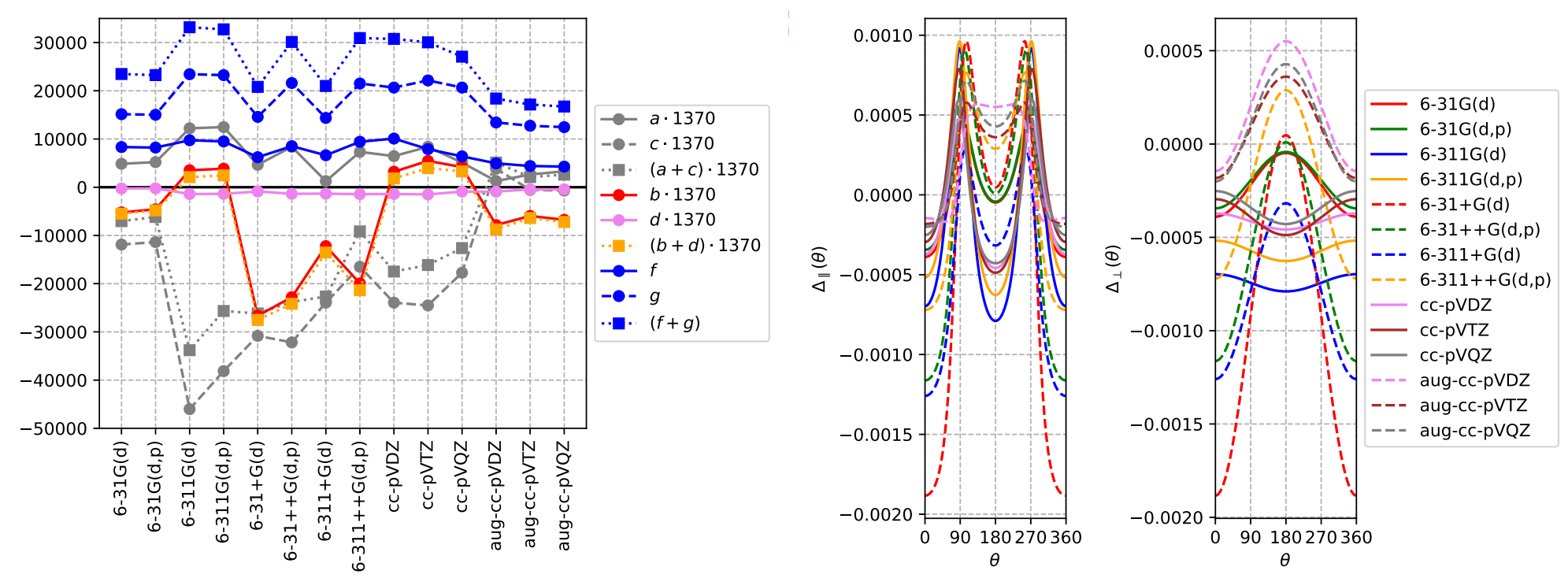
30000
20000
10000
0
−10000
−20000
−30000
−40000
−50000
6-31G(d)
6-31G(d,p)
6-311G(d)
6-311G(d,p)
6-31+G(d)
6-31++G(d,p)
6-311+G(d)
6-311++G(d,p)
cc-pVDZ
cc-pVTZ
cc-pVQZ
aug-cc-pVDZ
aug-cc-pVTZ
aug-cc-pVQZ
$a \cdot 1370$
$c \cdot 1370$
$(a+c) \cdot 1370$
$b \cdot 1370$
$d \cdot 1370$
$(b+d) \cdot 1370$
f
g
$(f+g)$
$\Delta_{\parallel}(\theta)$
0.0010
0.0005
0.0000
−0.0005
−0.0010
−0.0015
−0.0020
0
90
180
270
360
θ
$\Delta_{\perp}(\theta)$
0.0005
0.0000
−0.0005
−0.0010
−0.0015
−0.0020
6-31G(d)
6-31G(d,p)
6-311G(d)
6-311G(d,p)
6-31+G(d)
6-31++G(d,p)
6-311+G(d)
6-311++G(d,p)
cc-pVDZ
cc-pVTZ
cc-pVQZ
aug-cc-pVDZ
aug-cc-pVTZ
aug-cc-pVQZ